Final Report

Title: Radar Waveform Design of Undersampled Signals

Contract Number: FA5209-04-P-0447

AFOSR/AOARD Reference Number: AOARD-04-4046

AFOSR/AOARD Program Manager: Tae-Woo Park, Ph.D.

Period of Performance: 01 August 2004 – 01 August 2005

Submission Date: 19 April 2004

PI: Dr. Jim Schroeder

Co-PI: Dr. Murali Rangaswamy

Report Documentation Page

Form Approved
OMB No. 0704-0188

1. REPORT DATE	2. REPORT TYPE	3. DATES COVERED
27 JUL 2006	**Final Report (Technical)**	**08-07-2004 to 01-12-2005**

4. TITLE AND SUBTITLE
Radar Waveform Design of Undersampled Signals

5a. CONTRACT NUMBER
FA520904P0447

5b. GRANT NUMBER

5c. PROGRAM ELEMENT NUMBER

6. AUTHOR(S)
James Schroeder

5d. PROJECT NUMBER

5e. TASK NUMBER

5f. WORK UNIT NUMBER

7. PERFORMING ORGANIZATION NAME(S) AND ADDRESS(ES)
University of Adelaide,Univ of Adelaide, Engineering North,Adelaide SA 5000,AU,5000

8. PERFORMING ORGANIZATION REPORT NUMBER
AOARD-044046

9. SPONSORING/MONITORING AGENCY NAME(S) AND ADDRESS(ES)
The US Resarch Labolatory, AOARD/AFOSR, Unit 45002, APO, AP, 96337-5002

10. SPONSOR/MONITOR'S ACRONYM(S)
AOARD/AFOSR

11. SPONSOR/MONITOR'S REPORT NUMBER(S)
AOARD-044046

12. DISTRIBUTION/AVAILABILITY STATEMENT
Approved for public release; distribution unlimited

13. SUPPLEMENTARY NOTES

14. ABSTRACT
A primary goal in radar waveform design is to achieve a prescribed discrete time radar ambiguity function. Radar waveform design to meet a given ambiguity function specification is an important issue under the waveform diversity technology. Much of the development in this area is for continuous time signals. For the discrete time case, the sampling rate becomes an important design issue. On the one hand, too low of a sampling rate results in spectral aliasing, on the other hand, a sampling rate chosen higher than necessary increases the computational burden. We show in this project that aliased spectra, arising from sampling below the Nyquist rate, may be completely eliminated. We plot the effects of quantization noise and timing jitter for subjective evaluation.

15. SUBJECT TERMS

16. SECURITY CLASSIFICATION OF:			17. LIMITATION OF ABSTRACT	18. NUMBER OF PAGES	19a. NAME OF RESPONSIBLE PERSON
a. REPORT	b. ABSTRACT	c. THIS PAGE			
unclassified	**unclassified**	**unclassified**		**85**	

(2) **Objectives:** Briefly summarize the objectives of the research effort or the statement of work.

Statement of problem

We conjecture that a deterministic or random waveform that is sampled at a rate less than the classical Nyquist rate may be successfully reconstructed. Intuitively, additional information must be available at the sampling instants, in order to remove the aliased spectral components. For example, the additional information may be one or more higher order derivatives. Another possibility is a finite pulse that retains signal information during the entire pulse duration samples the signal. Yet another possibility is that two or more closely spaced samples are retained each sampling instant.

Our hypothesis is that a signal maybe sampled at one-half the Nyquist rate if two arbitrarily closely spaced samples are retained each sampling instant. In this case the system sampling rate could be cut in half, at the price of carrying two samples per sampling instant. There appears to be no theoretical reasons that the sampling rate cannot be further reduced.

Impact of the results of research

A primary goal in radar waveform design is to achieve a prescribed discrete time radar ambiguity function. Radar waveform design to meet a given ambiguity function specification is an important issue under the waveform diversity technology. Much of the development in this area is for continuous time signals. For the discrete time case, the sampling rate becomes an important design issue. On the one hand, too low of a sampling rate results in spectral aliasing, on the other hand, a sampling rate chosen higher than necessary increases the computational burden. We show in this research project that aliased spectra, arising from sampling below the Nyquist rate, may be completely eliminated in the absence of quantization noise and timing errors (jitter between doublet samples).

For the purpose of this research, we assume that the desired radar waveform is available. Since radar processing is done digitally, it is important to examine the effects of sampling the ambiguity function in the Delay-Doppler plane and study the resulting resolution trade-offs, reconstruction issues, and aliasing problems. The preliminary techniques developed in this research, and applied to the ambiguity function in this proposed research, should be quite useful in this context.

Approach

The approach for this research project is to apply the proposed aliased signal reconstruction algorithms to radar-like waveforms (i.e. random) then form the ambiguity function from the reconstructed waveform. We will show that, based on simulation results and mathematical derivation, that the reconstruction algorithm is valid for bandlimited random processes.

In addition to analytically proving convergence of the reconstruction algorithm, we present plots using Matlab-based simulation tools to illustrate the reconstruction errors when quantization noise and timing jitter are present. Both quantization noise and timing jitter will be real-world problems a radar design engineer would need to consider if these algorithms are used in on-line processing. For off-line waveform design purposes, noise sensitivities may be less of an issue.

(3) Status of effort: We have achieved our planned objectives to derive reconstruction equations to remove the aliasing when sampling (doublet impulse sampling) at ½ the Nyquist rate (Appendix A). The reconstruction equations have been demonstrated as valid for a random waveform by both simulation and mathematical proof (Appendix D). The effects of quantization noise and jitter have been illustrated subjectively over several dozens test cases (Appendix A). The Matlab M-files developed may be found in Appendix C. An interim paper presented at The Defense Applications of Signal Processing Workshop, www.dasp.ws, may be viewed in Appendix B.

During the course of this research project we identified a promising avenue to mitigate jitter noise. This research has not been pursued as part of this project, however, the basic idea is documented in the Appendix A conclusions section.

(4) Abstract:

A primary goal in radar waveform design is to achieve a prescribed discrete time radar ambiguity function. Radar waveform design to meet a given ambiguity function specification is an important issue under the waveform diversity technology. Much of the development in this area is for continuous time signals. For the discrete time case, the sampling rate becomes an important design issue. On the one hand, too low of a sampling rate results in spectral aliasing, on the other hand, a sampling rate chosen higher than necessary increases the computational burden. We show in this project that aliased spectra, arising from sampling below the Nyquist rate, may be completely eliminated. We plot the effects of quantization noise and timing jitter for subjective evaluation.

(5) Personnel Supported:

Dr. Jim Schroeder
School of Electrical and Electronic Engineering
The University of Adelaide
Adelaide, SA 5000
AUSTRALIA
schroeder@eleceng.adelaide.edu.au

Dr. Muralidhar Rangaswamy
Civ AFRL/SNHE
Hanscom AFB, MA 01731
Muralidhar.Rangaswamy@hanscom.af.mil

(6) Publications:

1) Defense Applications of Signal Processing Workshop, April 2005-11-12 re-printed in Appendix B
2) Conference paper submitted to ICASSP 2006
3) Planned journal length paper submission to DSP: A Review Journal by end of 2005, manuscript in preparation.

(7) Interactions: Please list:

(a) Participation and presentation at The Defense Applications of Signal Processing Workshop, The Homestead Resort, Utah, April 2005, http://www.dasp.ws
(b) Invited graduate seminar presentation to The School of Electrical and Computer Engineering, University of Iowa, Iowa City, Iowa.
(c) After further research the Hansom AFB AFRL may evaluate whether these reconstruction algorithms are useful for their LPI Diversity Waveform design efforts.

(8) New: None

(9) Honors/Awards: Dr. Murali Rangaswamy received an USAF AFRL Research Award.

(10) Archival Documentation: Appendix A contains the technical report documenting the research results. Appendix B is a reprint of the paper presented at DASP 2004/05 covering interim project results. Appendix C lists the Matlab M-

files. Appendix D contains a mathematical derivation showing that reconstructing a random process is error free in a mean square sense.

(11) Software and/or Hardware (if they are specified in the contract as part of final deliverables):

Matlab M-files located in Appendix C.

Appendix A: Technical Summary of Research Project "Radar Waveform Design of Undersampled Signals"

Background

A primary goal in radar waveform design is to achieve a prescribed discrete time radar ambiguity function. Radar waveform design to meet a given ambiguity function specification is an important issue under the waveform diversity technology. Much of the development in this area is for continuous time signals. For the discrete time case, the sampling rate becomes an important design issue. On the one hand, too low of a sampling rate results in spectral aliasing, on the other hand, a sampling rate chosen higher than necessary increases the computational burden. We show in this research project that aliased spectra, arising from sampling below the Nyquist rate, may be completely eliminated.

The radar ambiguity function based waveform design is complicated by the fact that for a given waveform, the ambiguity function can be readily calculated. However, given an ambiguity function specification, it is possible to have more than one waveform that meets the specification. For the purpose of this research project, we assume that the desired waveform is available. Since radar processing is done digitally, it is important to examine the effects of sampling the ambiguity function in the Delay-Doppler plane and study the resulting resolution trade-offs, reconstruction issues, and aliasing problems. The preliminary techniques developed in this project, and applied to the ambiguity function in this proposed research, should be quite useful in this context.

The goal of this research project was to apply the preliminary aliased signal reconstruction to radar waveform design against ambiguity plane constraints [19]. The radar receiver discrete time matched filter computational complexity may be potential reduced by implementing the signal restoration algorithm summarised in this report. We originally hypothesised, based on early simulation results, that the reconstruction algorithm is valid for bandlimited random processes. Subsequently, we proved analytically that exact reconstruction of bandlimited random processes is possible. This is an important result since modern radar waveform design involves the use of pseudorandom coding for pulse compression and LPI/LPD waveforms.

Sampling Theory

A generalised version of the Nyquist sampling theorem admits sampling at an average rate equal to twice the highest frequency component of the sampled signal. For example, we may envision a sampling structure wherein a pair of closely spaced impulses perform the signal sampling, each impulse pair sampling the signal at one-half the minimum rate required for ideal impulse sampling. In this report we derive a frequency domain restoration algorithm and its corresponding time domain interpolation formula, and analytically quantify the effect of impulse pair spacing on the numerical conditioning of

the restoration algorithm. Simulations results are provided to demonstrate reconstruction of an ideal bandlimited deterministic tests signal and a bandlimited random process.

Research into representing a function by its sample values, and development of the corresponding interpolation formulas, enjoys a rich history [1-11]. Representations may be chosen, e.g. by use of Fourier series coefficients, that do not restrict the frequency domain support. Although Fourier coefficients are attractive for many reasons, a variety of interpolation functions have been invoked [1,3,4,7]. Other convenient representations, e.g. use of the function sample values directly, require the function to be bandlimited. Bandlimited functions that are sampled at less than the Nyquist rate [2] exhibit a distortion termed aliasing, however, many situations allow the aliasing to be eliminated or reduced if additional information is available at the sampling instants [8,9,11,12,15-18].

Staggered Sampling Theory

Although so called 'Staggered Sampling Theory," [c.f. 20-35 as a small reference sample] is outside the scope of this study, we note the parallels to our work. Staggered sampling is widely used in the high- speed oscilloscope industry so that two or more parallel streams of sampled data, offset in time, may be used to lower the system-sampling rate.

Staggered sampling is useful for several applications such as sensor networks, analog-to-digital converter (ADC), and sampling high bandwidth analog signals.

Staggered sampled ADCs are an alternative for parallelizing the sampling task over several converters. Such a system may provide a relatively high sampling rate with component ADCs operating at lower rates. The issues with staggered sampling tend to be the difficulty of maintaining close timing accuracy between the sample streams and quantization errors from finite arithmetic. Conventional staggered sampling theory makes use of filter bank theory with required up and down sampling converters that may be a disadvantage.

In this research we provide an alternative formulation that admits sampling directly at ½ the Nyquist rate without any required up and down sampling. Although we restrict our attention to the two-channel case, there is no mathematical reason the theory cannot be extended to a greater number of channels (for example we could sample at ¼ the Nyquist rate and carry four closely spaced samples each system sampling instant).

Impulse-doublet Sampling

A generalised version of the Nyquist sampling theorem [8] admits sampling at an average rate equal to twice the highest frequency component of the sampled signal. For example, we may envision a sampling structure wherein a pair of closely spaced impulses perform the signal sampling, each impulse pair sampling the signal at one-half the minimum rate required for ideal impulse sampling. Let $f(t)$ be a low pass signal with bandwidth $f_c = W$ Hz that is sampled by the function

$$p(t) = \delta(t + \tau/2) + \delta(t - \tau/2)$$

at a rate $f_s = f_c = 1/T$ Hz, $0 < \tau << T/2$. We assume that f(t) is real so that the sampled spectrum is Hermitian, and may be restored using positive frequencies only. The aliased spectrum, $F^*(\omega)$ over $0 \leq f \leq f_c$ (using $\omega = 2\pi f$ to avoid notational difficulties) is given by

$$F^*(\omega) = A_0\, F(\omega) + A_1 F(\omega - \omega_s)$$

where

$$A_m = (2/T)\cos(m\omega_c\tau/2)$$

as shown in Figure 1.

Reconstruction Equations

We next derive a frequency domain restoration algorithm and its corresponding time domain interpolation formula.

The key mathematical manipulations will be shown.

$$F^*(\omega) = A_0\, F(\omega) + A_1 F(\omega - \omega_S)\ ,\ 0 \leq \omega \leq \omega_C \text{ Let } \omega_0 = \omega_C/2$$

$$F^*(\omega_0) = A_0\, F(\omega_0) + A_1 F(\omega_0 - \omega_S)$$

Assume f(t) is real valued, then

$$F(-\omega) = F^\wedge(\omega)$$

$$F^*(\omega_0) = A_0\, F(\omega_0) + A_1 F^\wedge(\omega_S - \omega_0)$$

But $\omega_S = 2\,\omega_0$

Therefore,

$$F^*(\omega_0) = A_0\, F(\omega_0) + A_1 F^\wedge(\omega_0)$$

$$F^*(\omega_0) = F_r^*(\omega_0) + jF_i^*(\omega_0)$$

and

$$F(\omega_0) = F_r(\omega_0) + jF_i\,(\omega_0)$$

It follows that

$$F_r^*(\omega 0) + jF_i^*(\omega 0) = A0[F_r(\omega 0) + jF_i\,(\omega 0)] + A1[F_r(\omega 0) - jF_i\,(\omega 0)]$$

Equating the real and imaginary parts, we have

$$F_r^*(\omega 0) = A0F_r(\omega 0) + A1\;F_r\,(\omega 0)$$

$$F_i^*(\omega 0) = A0F_i(\omega 0) - A1\;F_i\,(\omega 0)$$

Now, consider

$$\omega = \omega 0 \;+/-\; \Delta\omega$$

in the aliased overlap region

$$F^*(\omega 0 \;+/-\; \Delta\omega) = A0\;F(\omega 0 \;+/-\; \Delta\omega) + A1F(\omega 0 \;+/-\; \Delta\omega\;\; - \omega_s),$$

$$0 \le \omega \le \omega_c$$

Let

$$\omega 0 = \omega_c/2 \text{ or } \omega_s = 2\omega 0$$

$$F^*(\omega 0 \;+/-\; \Delta\omega) = A0\;F(\omega 0{+/-}\;\Delta\omega) + A1F(-\omega 0 \;+/-\; \Delta\omega)$$

Assume f(t) is real valued, then

$$F(-\omega) = F\hat{}(\omega)$$

and

$$F^*(\omega 0 \;+/-\; \Delta\omega) = A0\;F(\omega 0{+/-}\;\Delta\omega) + A1F\hat{}(\omega 0 \;-/+\; \Delta\omega)$$

Equating Real and Imaginary parts results in

$$Fr^*(\omega 0 \;+/-\; \Delta\omega) = A0\;Fr(\omega 0{+/-}\;\Delta\omega) + A1Fr\hat{}(\omega 0 \;-/+\; \Delta\omega)$$

$$Fi^*(\omega 0 \;+/-\; \Delta\omega) = A0\;Fi(\omega 0{+/-}\;\Delta\omega) - A1Fi\hat{}(\omega 0 \;-/+\; \Delta\omega)$$

Real part:

$$Fr^*(\omega 0 + \Delta\omega) = A0\;Fr(\omega 0{+}\;\Delta\omega) + A1Fr\hat{}(\omega 0 - \Delta\omega)$$

$$Fr^*(\omega 0 - \Delta\omega) = A0\;Fr(\omega 0{-}\;\Delta\omega) + A1Fr\hat{}(\omega 0 + \Delta\omega)$$

Imaginary part:

$$Fi^*(\omega_0 + \Delta\omega) = A_0\, Fi(\omega_0 + \Delta\omega) - A_1 Fi\hat{}(\omega_0 - \Delta\omega)$$

$$Fi^*(\omega_0 - \Delta\omega) = A_0\, Fi(\omega_0 - \Delta\omega) - A_1 Fi\hat{}(\omega_0 + \Delta\omega)$$

Solution of the simultaneous equations leads to

$$Fr(\omega_0 +/- \Delta\omega) = [A_0\, Fr^*(\omega_0 +/- \Delta\omega) - A_1 Fr^*(\omega_0 -/+ \Delta\omega)\,]/\,[A_0^2 - A_1^2]$$

$$Fi(\omega_0 +/- \Delta\omega) = [A_0\, Fi^*(\omega_0 +/- \Delta\omega) + A_1 Fi^*(\omega_0 -/+ \Delta\omega)]\,/\,[A_0^2 - A_1^2]$$

Let $\Delta\omega$ be some arbitrary frequency offset from ω_0

$$F^*(\omega_0 + \Delta\omega) = A_0\, F(\omega_0 + \Delta\omega) + A_1 F(\omega_0 - \Delta\omega)$$

$$F^*(\omega_0 - \Delta\omega) = A_0\, F(\omega_0 - \Delta\omega) + A_1 F(\omega_0 + \Delta\omega)$$

The derivation, by straightforward manipulation of the aliased spectral equations as just derived manually, may be summarized compactly as

$$F = A^{-1}F^*$$

with

$$A = \begin{bmatrix} A_0 & A_1 \\ A_1 & A_0 \end{bmatrix}$$

$$F = \begin{bmatrix} F(\omega_0 + \Delta\omega) \\ F(\omega_0 - \Delta\omega) \end{bmatrix}$$

$$F^* = \begin{bmatrix} F^*(\omega_0 + \Delta\omega) \\ F^*(\omega_0 - \Delta\omega) \end{bmatrix}$$

where $\omega_0 = \omega_c/2$, and $\Delta\omega$ is an arbitrary frequency offset from ω_0.

And re-substituting

$$\omega_s = 2\ \omega_0$$

$$F(\omega) = A_0/(A_0^2 - A_1^2)\ F^*(\omega) - A_1/\ (A_0^2 - A_1^2)\ F^*(\omega - \omega_s)$$

$$0 \leq \omega \leq \omega_c$$

Upon application of a brick wall ideal filter, $G(\omega) = 1$, $0 \leq \omega \leq \omega_c$, to the positive frequency components defined by the frequency domain reconstruction formula, the time domain interpolation equation follows directly as

$$F(\omega) = A_0/(A_0^2 - A_1^2)\ F^*(\omega) - A_1/\ (A_0^2 - A_1^2)\ F^*(\omega - \omega_s)$$

$$0 \leq \omega \leq \omega_c$$

$$f(t) = 2\mathrm{Re}\{g(t)*[A_0/(A_0^2 - A_1^2)\ f^*(t) - A_1/\ (A_0^2 - A_1^2)\ f^*(t)\ e^{j\ \omega s t y}]\}$$

$$\text{where } g(t) = \mathcal{F}^{-1}\{G(\omega)\ \}$$

leads to

$$f(t) = 2\,\mathrm{Re}\left\{\sum_{n=-\infty}^{n=+\infty}\begin{bmatrix} x(nT+\tau/2)g(t-nT+\tau/2) \\ +\,x(nT-\tau/2)g(t-nT-\tau/2) \end{bmatrix}\right\}$$

with

$$g(t) = \frac{W\sin(\pi Wt)}{\pi Wt}e^{j\pi Wt}$$

$$x(t) = \frac{A_0 - A_1 e^{j2\pi Wt}}{A_0^2 - A_1^2}f^*(t)$$

where $f^*(t)$ is the sampled version of f(t).

Alternatively, the aliasing could be removed in the discrete frequency domain. A frequency domain reconstruction might be attractive computationally, however, careful consideration of windowing effects would be required. Another advantage may be that diagonal loading of the matrix equations could lead to a Maximum Likelihood solution to mitigate jitter noise effects. Such topics are outside the scope of this investigation.

We may quantify the effect of impulse pair spacing on the numerical conditioning of the restoration algorithm. The eigenvalues of matrix A are A_0 +/- A_1, A_0, $A_1 > 0$, $A_1 < A_0$; therefore the matrix Condition Number of A is given by

$$C.N. = \frac{A_0 + A_1}{A_0 - A_1}$$

$$A_0 = \frac{2}{T}$$

$$A_1 = \frac{2}{T}\cos(\pi W \tau).$$

We observe that:

- As τ approaches zero the C.N. $\to \infty$ as we expect, i.e., matrix A is singular, and no reconstruction is possible
- As τ approaches T/2 the C.N. $\to 1$, i.e., $A_1 = 0$, the aliasing is zero, and conventional ideal impulse sampling at the Nyquist rate obtains in the limit
- For $0 < \tau < T/2$ numerical stability of the time domain interpolation formula or the frequency domain alias removal algorithms are clearly a function of the impulse-doublet spacing.

Simulation Results

The following simulations illustrate that reconstruction is possible with the aliased components removed. We consider an ideal bandlimited test signal, the "Sinc Function," as well as a more realistic signal modelling a bandlimited random process.

Figure 2. illustrates the results of sampling a .1 Hz bandwidth "Sinc Function," at .1 Hz. We reconstruct 100 points, with each reconstructed point estimated from a 500-point summation. The impulse doublet has width .01 Second for this example. No noise has been added.

The next two examples illustrates that reconstruction of a random process appears possible (indeed we have been able to prove convergence). White Gaussian Noise was filtered to .1 Hz with a 500 tap FIR filter. The sampling rate is .1 Hz. As for the previous example, the impulse doublet width is set arbitrarily to .01 second. In Figure 3. we illustrate the reconstruction of this random process. Figure 4. shows reconstruction of a noise-like waveform, 16-QAM with added noise. Although not shown, reconstruction of 16-QAM without added noise is error free. In fact all waveforms tried, even a pure

sinusoid (bandpass rather than low pass) reconstructed error free without added noise, somewhat a surprise as we assumed low pass spectra during the derivation.

The next simulations demonstrate the effects of quantization noise and timing jitter between the staggered samples represented by the doublet impulse pair. We also illustrate the effects of reconstruction inaccuracies due to quantization on an ambiguity function, widely used in radar signal design [19], computed from a Sinc function.

Figures 5. – 9. illustrate the degrading effects on computing an ambiguity function of the Sinc function for 8 bit, 16 bit, and 32 bit quantization. The Sinc function is chosen as an ideal low pass waveform that possessing infinite time-domain support, thus it's a difficult signal to reconstruct. The results are not surprising although might have desired less reconstruction error for 16 bit arithmetic. The 32 bit quantization results in a zero error reconstruction.

It is easier to view the degradation due to jitter and quantization direction on the reconstructed Sinc function rather than adding the extra transformation into the ambiguity plane. Therefore, the remaining simulations focus on the time domain reconstructed Sinc function and several example Power Spectral Densities (PSDs) to show the impact in frequency.

For the results in Figures 10. – 18. we fix the quantization at 16 bits, and then allow the spacing between the impulse pair to vary. Recall that we showed the numerical ill conditioning directly related to impulse pair spacing with reduced spacing resulting in greater ill conditioning.

A spacing of .001 seconds is disastrous, .005 seconds much improved, and degradation just noticeable at a spacing of .01 seconds. At a spacing of .025 – 1.0 seconds the reconstruction error is zero. Whether this degradation is acceptable would require analysis and simulation based upon a specific radar system.

Fortunately, from Figures 19. – 21., we see that switching to 32 bit quantization removes any error even at the closely spaced case of .001 seconds.

Less fortunately, although unsurprising, in Figures 22. – 26. we note that the results for 8 bit quantization are unacceptable.

Figures 27. and 28. show the effect of jitter with a doublet spacing of .01 second, and jitter variances of .001 and .005 with predictable results. The variance level was chosen to illustrate an acceptable degradation and unacceptable degradation rather than any connection to a technical specification. Again, whether these jitter levels are acceptable or practical requires simulation based upon real-world hardware specifications.

Finally, in Figures 29. – 31. we show the effects of jitter on the PSD of the reconstructed Sinc function. Although passband distortion is apparent the major component of the effects of jitter appear to be in the level of the out of band spectral energy. This result

bears some future caution and study into the effects of timing jitter on the reconstruction equation accuracy.

Conclusions and Further Study

We have summarised time domain and frequency domain restoration algorithms for a signal sampled by a periodic impulse-doublet at a rate equal to one-half the conventional Nyquist rate. The numerical stability of the proposed solution is a function of the C.N. of matrix A, directly related to the impulse-doublet spacing. The reconstruction equations become ill posed as $\tau \rightarrow 0$. We presented simulation results that demonstrate the accuracy of the time domain reconstruction equations with and without noise added to the samples, time domain jitter between the staggered samples, and with quantization noise added. We note that there does not appear to be any mathematical reason the sampling rate cannot be reduced, and the additional aliased spectra restored in an extended solution to the simplified case we considered here of first order aliasing.

The aliasing could also be removed in the discrete frequency domain. A frequency domain reconstruction might be attractive computationally, however, careful consideration of windowing effects would be required. Another advantage may be that diagonal loading of the matrix equations could lead to a Maximum Likelihood solution to mitigate jitter noise effects. Such topics are outside the scope of this investigation.

Based upon the simulation results applied to reconstructing a bandlimited random process, we came to believe that the restoration equations presented here are indeed valid for bandlimited random processes. Indeed, we have demonstrated mathematically in this research that reconstruction of an aliased bandlimited random process is possible in a "Limit in the Mean" sense.

The effect of A/D quantisation noise, and sample timing jitter, should be quantified objectively via simulation for specific hardware and systems, before the potential use of these reconstruction algorithms can be considered for an operational radar system. For off-line waveform design purposes, noise sensitivities may be less of an issue.

References

[1] E.T. Whitaker, "On the functions which are represented by the expansion of interpolating theory," Proc. Roy. Soc. Edinburgh, vol. 35, pp. 181-194, 1915.

[2] H. Nyquist, "Certain topics in telegraph transmission theory," AIEE Trans., vol. 47, pp.617-644, 1928.

[3] J.M. Whitaker, "The Fourier theory of cardinal functions," Proc. Math Soc. Edinburgh, vol. 1, pp. 169-176, 1929.

[4] D. Gabor, "Theory of communications," J. Inst. Elec. Eng. Vol. 93, no. 3, pp. 429-457, 1946.

[5] C.E. Shannon, “Communications in the presence of noise,” Proc. IRE., vol. 37, pp. 10-21, Jan. 1949.

[6] H.S. Black, Modulation Theory, New York: van Nostrand, 1953.

[7] J. Zak, “Finite translations in solid-state physics,” Phys. Rev. Lett., vol. 19, pp. 1385-1387, 1967.

[8] A. Papoulis, Systems and transforms with applications in optics, New York: McGraw Hill, 1968.

[9] J.M. Wozencraft and I.M. Jacobs, “Principles of communication engineering, New York: Wiley, 1965.

[10] A.J. Jerri, “The Shannon sampling theorem – Its various extensions and applications: A tutorial review,” Proc. IEEE, vol. 65, no. 11, pp. 1565-1598, November, 1977.

[11] A. Nathan, “On sampling a function and its derivatives,” Information and Control, Academic Press, vol. 22, pp. 172-182, 1973.

[12] R.J. Marks, “Restoration of a continuously sampled band-limited signal from aliased data,” IEEE ASSP, vol. ASSP-30, no. 5, pp. 937-942, December 1982.

[13] K.F. Cheung, and R.J. Marks, “Ill-posed sampling theorems,” IEEE Trans. Ckts. Sys., vol. CAS-32, no.5, May 1985.

[14] X-G Xia, and Z. Zhang, “On sampling theorem, wavelets, and wavelet transforms,” IEEE Trans. SP, vol. 41, no. 12, December 1993.

[15] P.E. Pace, R.E. Leino, and D. Styer, “Use of the symmetrical number system in resolving single-frequency undersampling aliases,” IEEE Trans. SP, vol. 45, no. 5, pp. 1153-1160, May 1997.

[16] D. Seidner, and M. Feder, “Noise amplification of periodic nonuniform sampling,” IEEE Trans. SP, vol. 48, no. 1, pp. 275-277, January 2000.

[17] M.B. Matthews, “On the linear minimum-mean-squared-error estimation of an undersampled wide-sense stationary random process,” IEEE Trans. SP, vol. 48, no. 1, pp. 272-275, January 2000.

[18] J. Angeby, “Aliasing of polynomial-phase signals,” IEEE Trans. SP, vol. 48, no. 5, pp. 1488-1491, May 2000.

[19] M.I. Skolnik, “Introduction to Radar Systems,” McGraw-Hill, New York, 1980.

[20] J. Elbornsson, F. Gustafsson, and J.-E. Eklund, Amplitude and gain error inuence on time error estimation algorithm for time interleaved A/D converter system, Proc. IEEE ICASSP, pages 1281-1284, 2002.

[21] K. Dyer, D. Fu, P. Hurst, and S. Lewis, A comparison of monolithic background calibration in two time-interleaved analog-to-digital converters, Proc. IEEE ICASSP, pages 13-16, 1998.

[22] F.J. Beutler, Error-free recovery of signals from irregularly spaced samples, SIAM Rev., 8:328-335, July 1966.

[23] W.C. Black and D.A. Hodges. Time interleaved converter arrays. IEEE Journal of Solid-State Circuits, 15:1022{1029, December 1980.

[24] J. P. Boyle and R. L. Dykstra, A method for finding projections onto the intersection of convex sets in Hilbert spaces, Advances in Order Restricted Inference, 37:28-47, 1985.

[25] Y. C. Eldar and A. V. Oppenheim, Filterbank reconstruction of bandlimited signals from nonuniform and generalized samples, IEEE Trans. Signal Processing, 48(10):2864-2875, October 2000.

[26] M. Feder, Statistical Signal Processing using a class of Iterative Estimation Algorithms, PhD thesis, Massachusetts Institute of Technology, 1987.

[27] H. Jin and E. K. F. Lee, A digital-background calibration technique for minimizing timing-error effects in time-interleaved ADCs, IEEE Trans. Circuits, Systems II, 47:603-613, July 2000.

[28] C. H. Knapp and G. C. Carter, The generalized correlation method for estimation of time delay, IEEE Trans. Acoust., Speech, Signal Processing, pages 320-327, August 1976.

[29] N. M. Laird, A. P. Dempster, and D. B. Rubin, Maximum likelihood from incomplete data via the EM algorithm, Ann. Roy. Stat. Soc., pages 1-38, December 1977.

[30] P. Marziliano and M. Vetterli, Reconstruction of irregularly sampled discrete-time bandlimited signal with unknown sampling locations, IEEE Trans. Signal Processing, 48(12):3462-3471, December 2000.

[31] A. V. Oppenheim, R. W. Schafer, and J. R. Buck, Discrete-Time Signal Processing, Prentice Hall, 1999.

[32] M. Patriksson, Partial linearization methods in nonlinear programming, Journal of Optimization Theory and Applications, 78:227-246, 1993.

[33] H. L. Van Trees, Detection, Estimation, and Modulation Theory, Pt. I, John Wiley and Sons, 1968.

[34] C. Vogel, Comprehensive, error analysis of combined channel mismatch effects in time interleaved ADCs. In Proc. IEEE IMTF, pages 733-738, 2003.

[35] K. Yao and J. B. Thomas, On some stability and interpolatory properties of nonuniform sampling expansions, IEEE Trans. Circuit Theory, pages 404-408, December 1967.

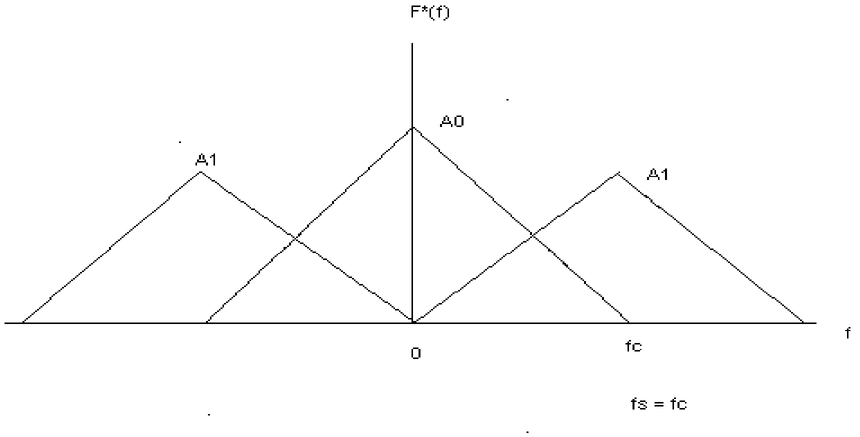

Figure 1. Aliased Spectrum Sampled at One-Half the Nyquist Rate

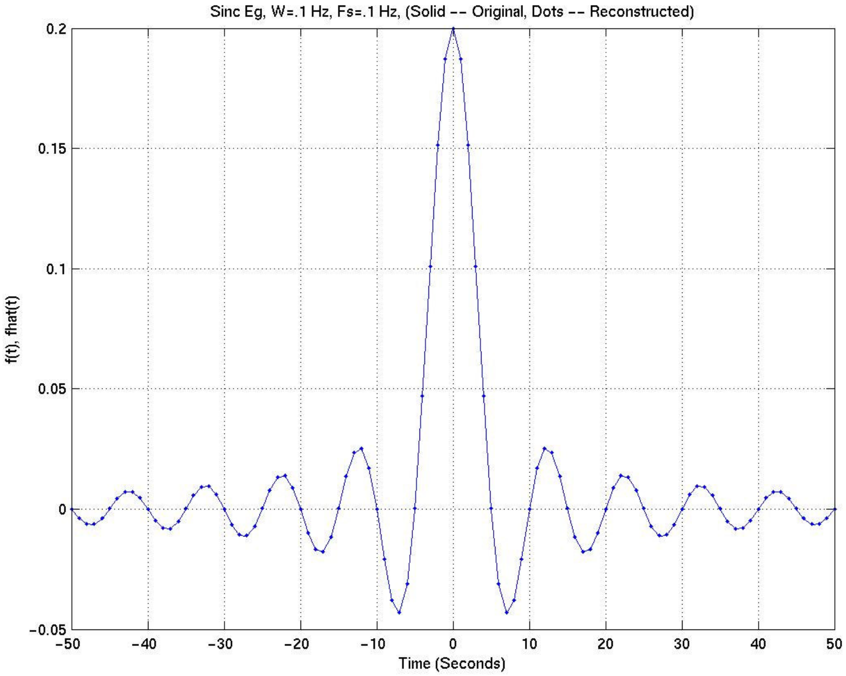

Figure 2. Reconstructed "Sinc Function," 500 Samples Used, τ = .01 Sec, No Added Noise

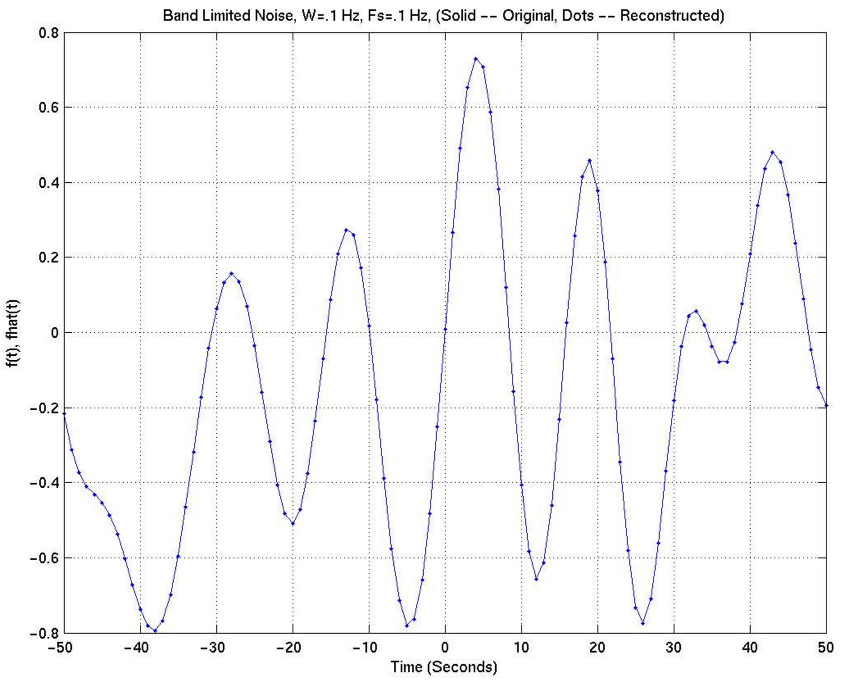

Figure 3.

Figure 3. Reconstructed Bandlimited Noise, $\tau = .01$ Second

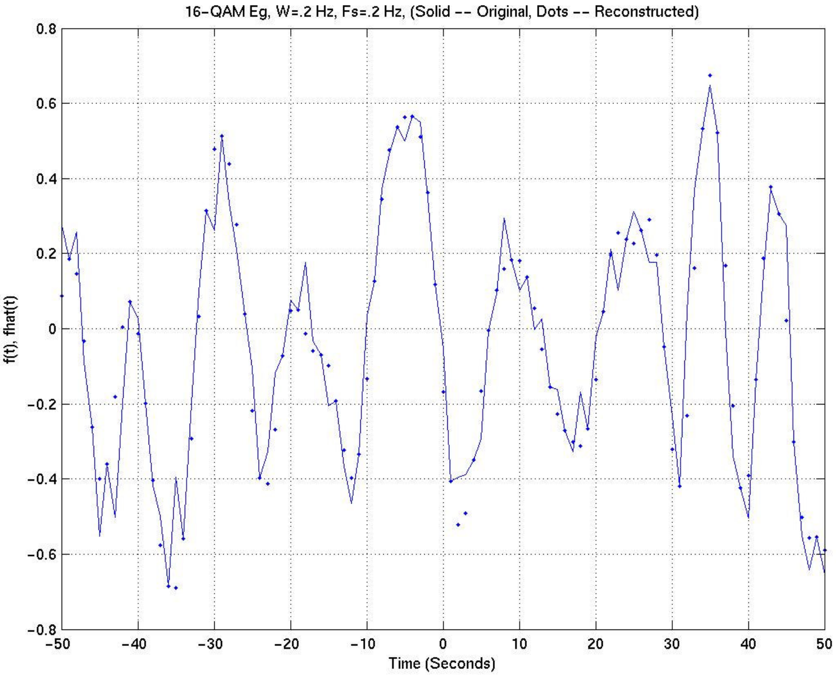

Figure 4. Reconstructed 16-QAM With Additive Noise, $\tau = 2$ Seconds, Noise Variance = 10^{-2}

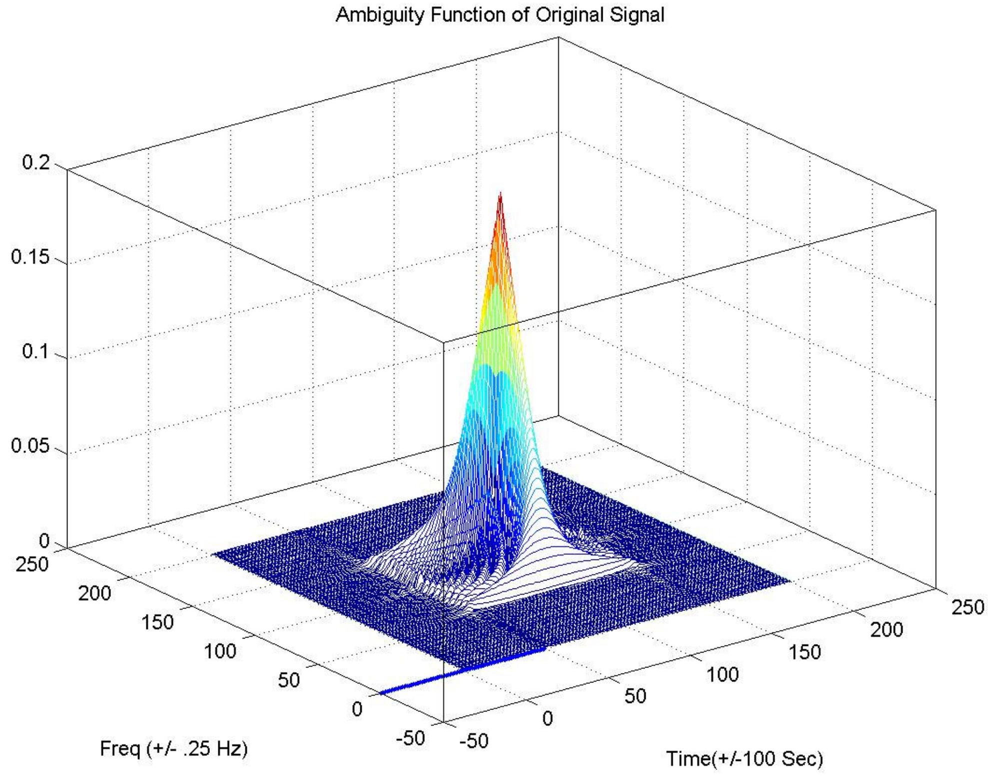

Figure 5. Ambiguity Function of Sinc Function, No Noise

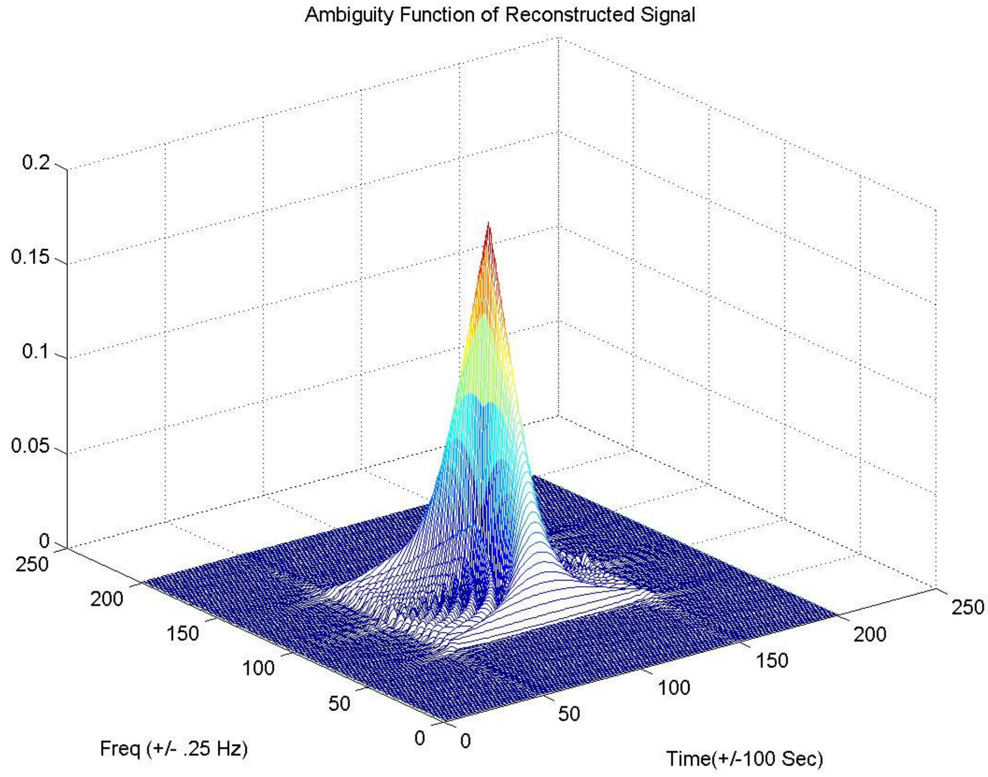

Figure 6. Ambiguity Function of Reconstructed Sinc Function, No Noise

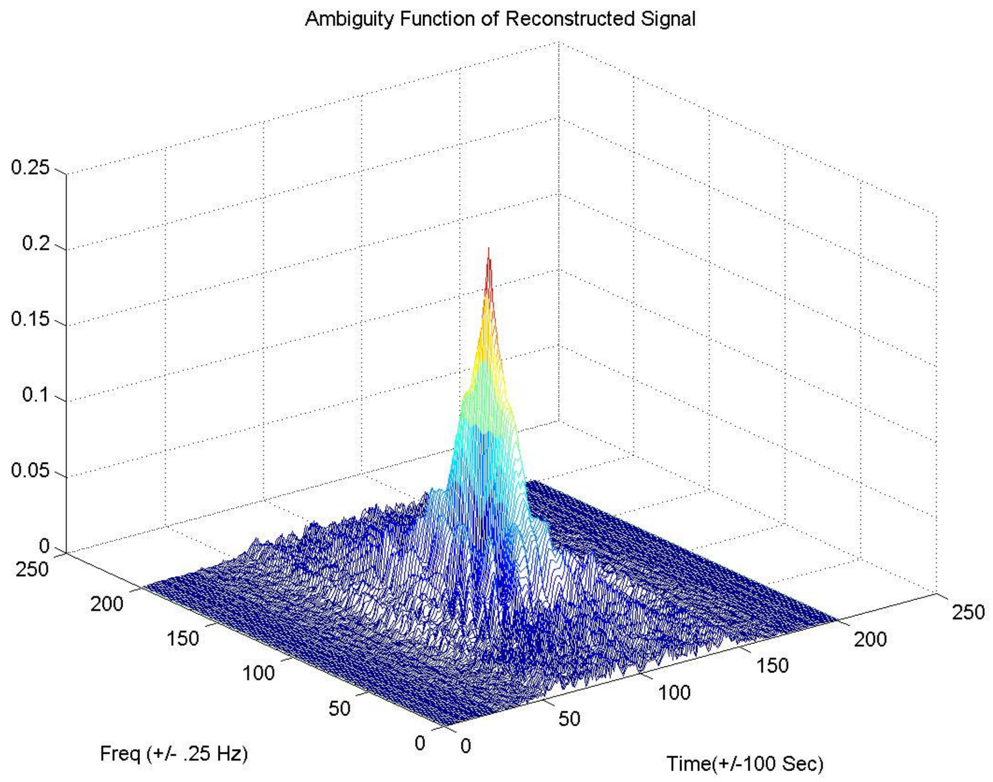

Figure 7. Ambiguity Function of Reconstructed Sinc Function, 8 Bit Quantization, tau = 1.0

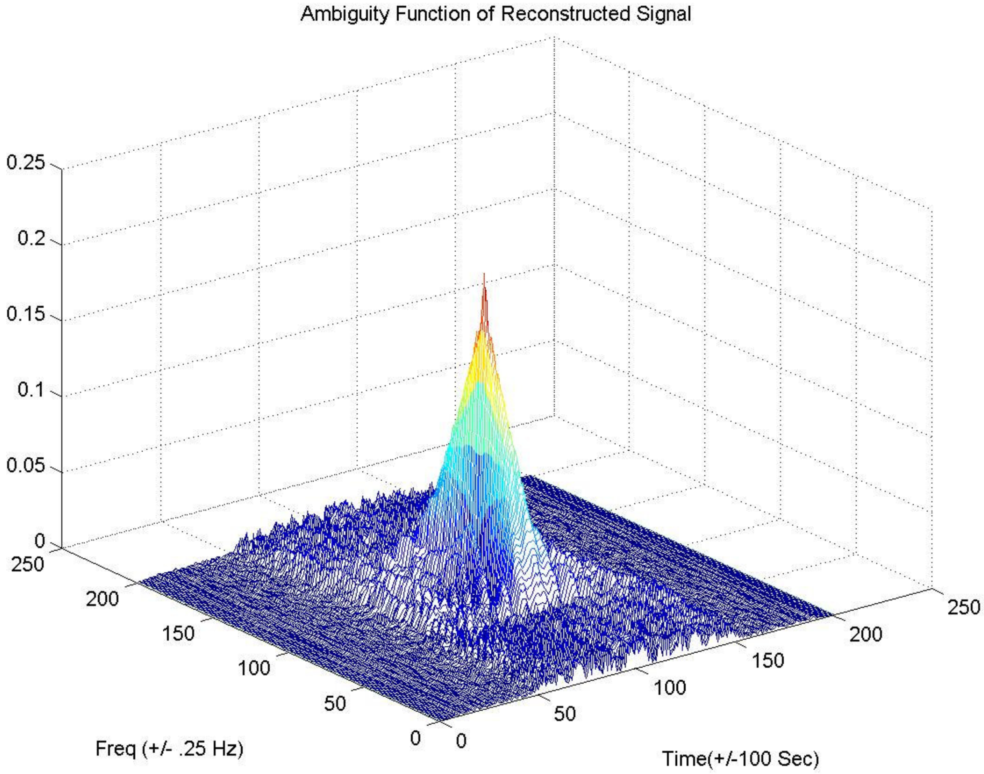

Figure 8. Ambiguity Function of Reconstructed Sinc Function, 16 Bit Quantization

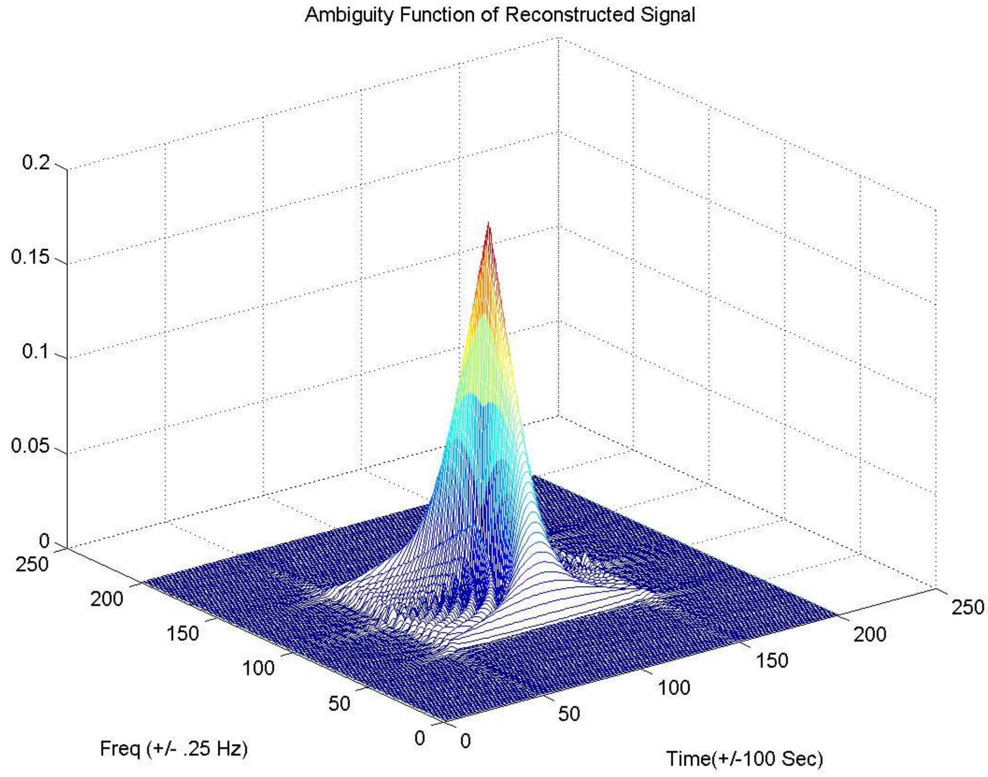

Figure 9. Ambiguity Function of Sinc Function, 32 Bit Quantization

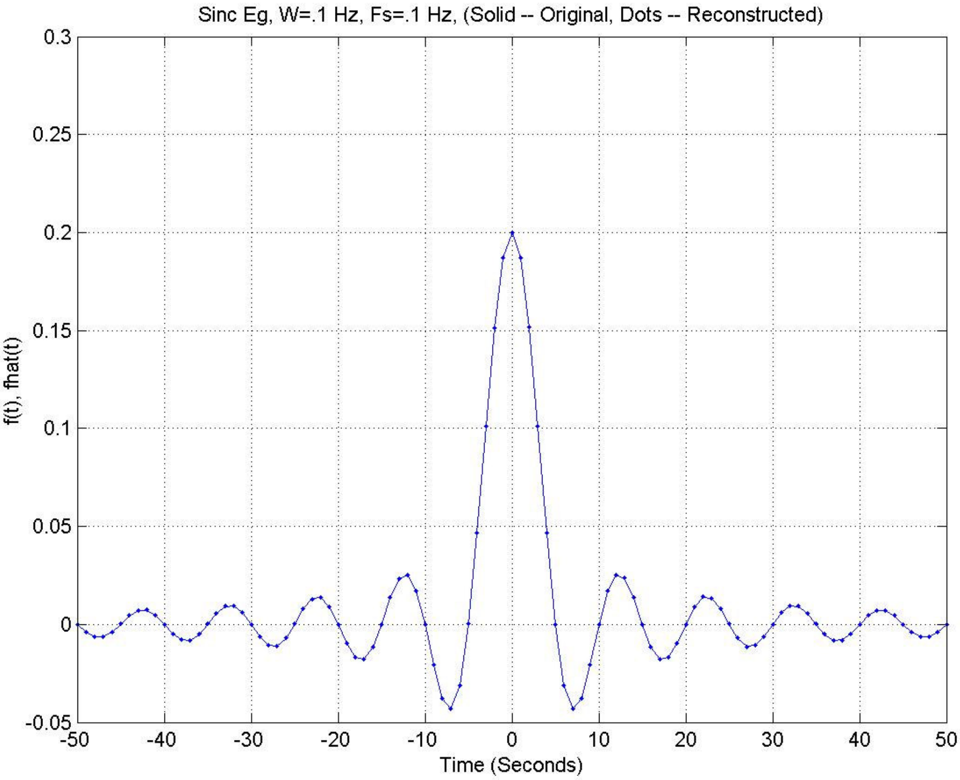

Figure 10. Reconstructed Sinc Function, 16 Bit Quantization

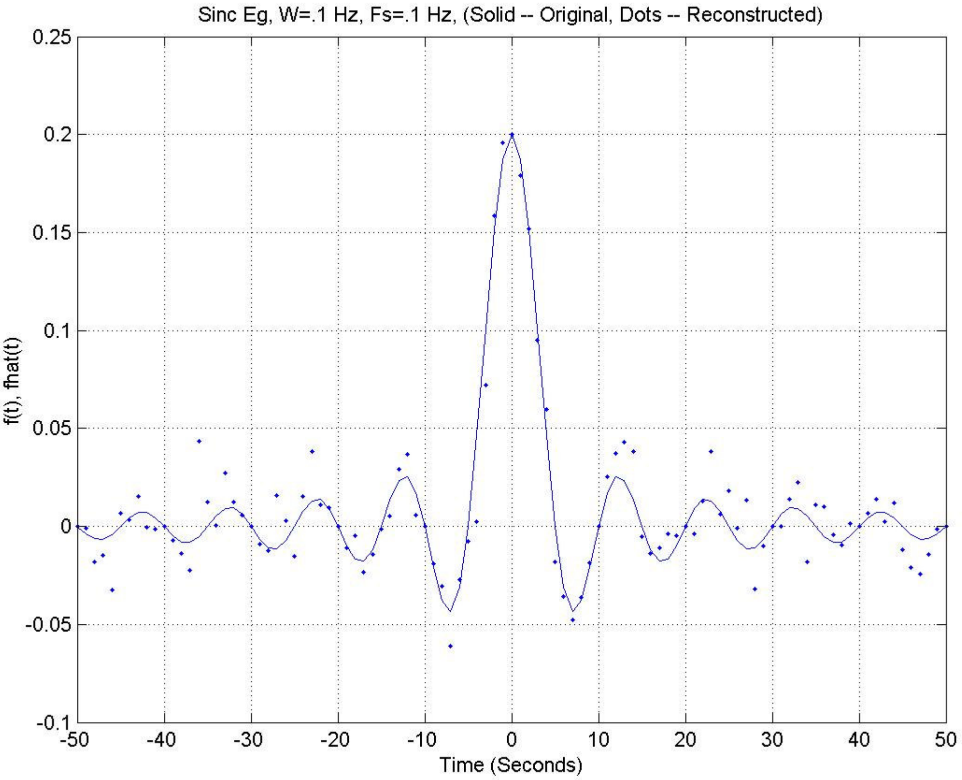

Figure 11. Reconstructed Sinc Function, 16 Bit Quantizatiom, Tau = .001 Sec

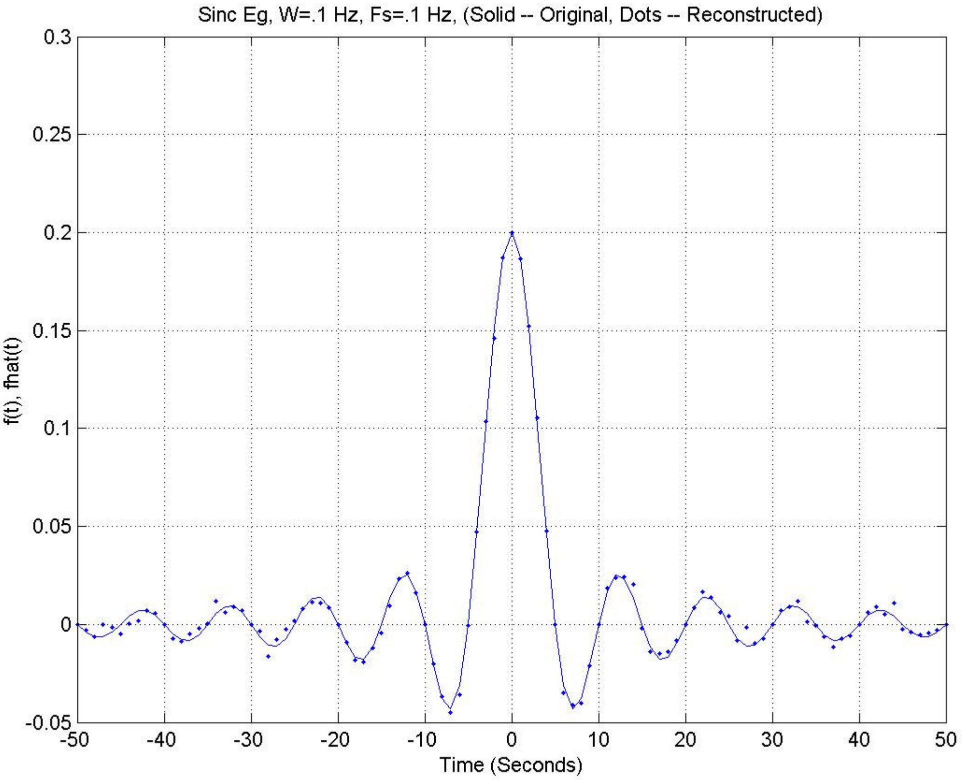

Figure 12. Reconstructed Sinc Function, 16 Bit Quantization, Tau = .005 Sec

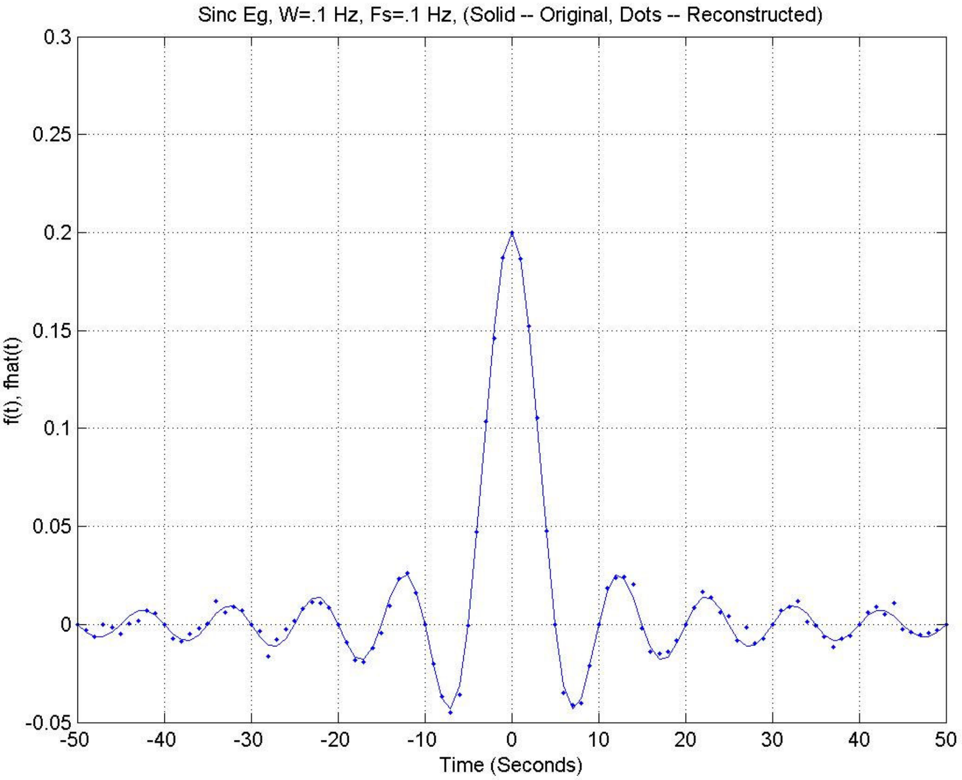

Figure 13. Reconstructed Sinc Function, 16 Bit Quantization, Tau = .005 Sec

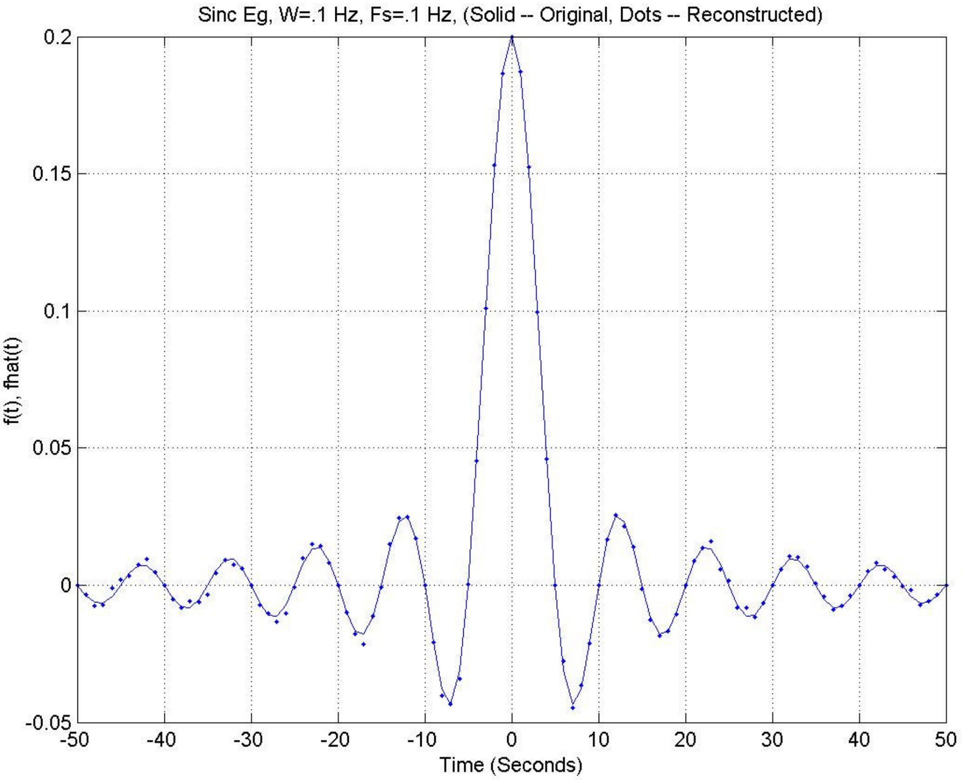

Figure 14. Reconstructed Sinc Function, 16 Bit Quantization, Tau = .01 Sec

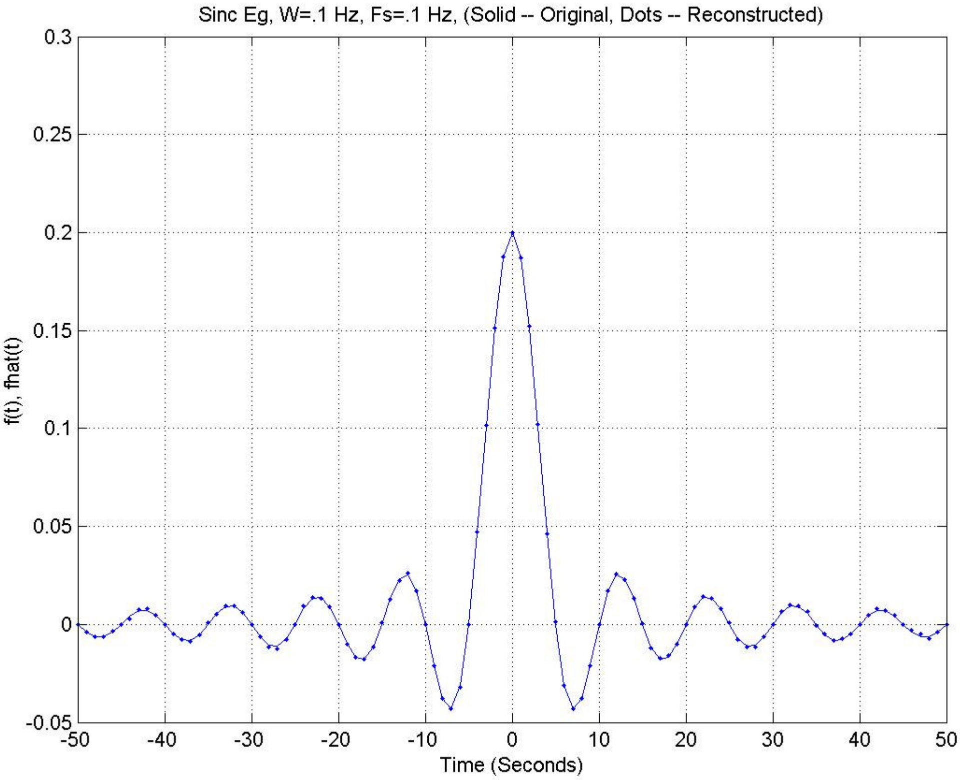

Figure 15. Reconstructed Sinc Function, 16 Bit Quantization, Tau = .025 Sec

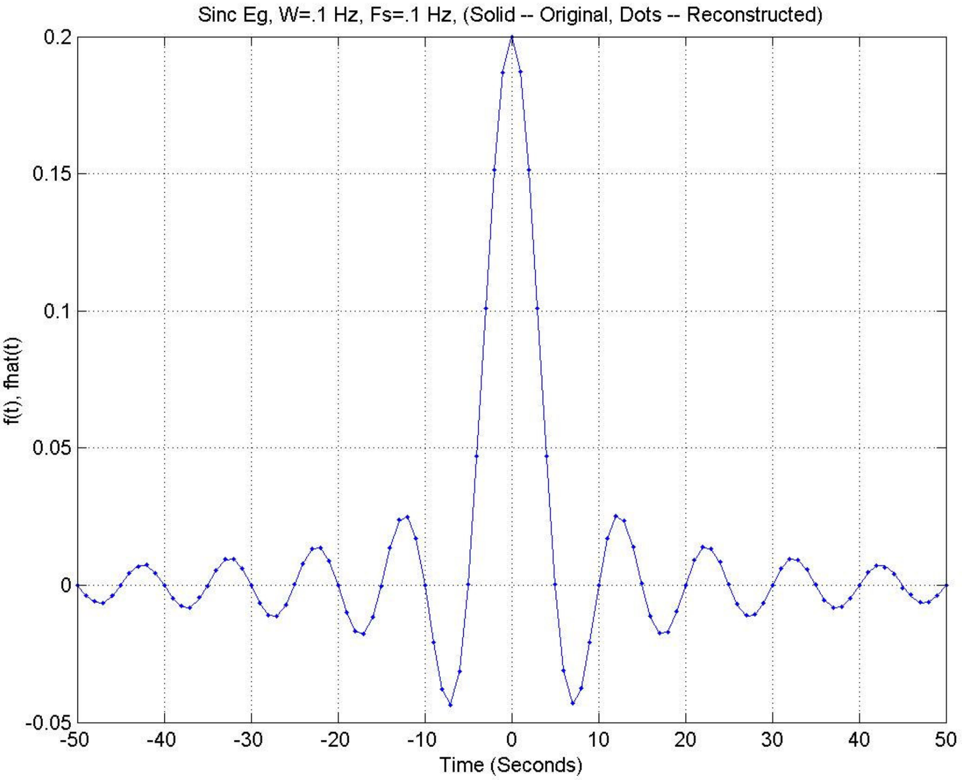

Figure 16. Reconstructed Sinc Function, 16 Bit Quantization, Tau = .025 Sec

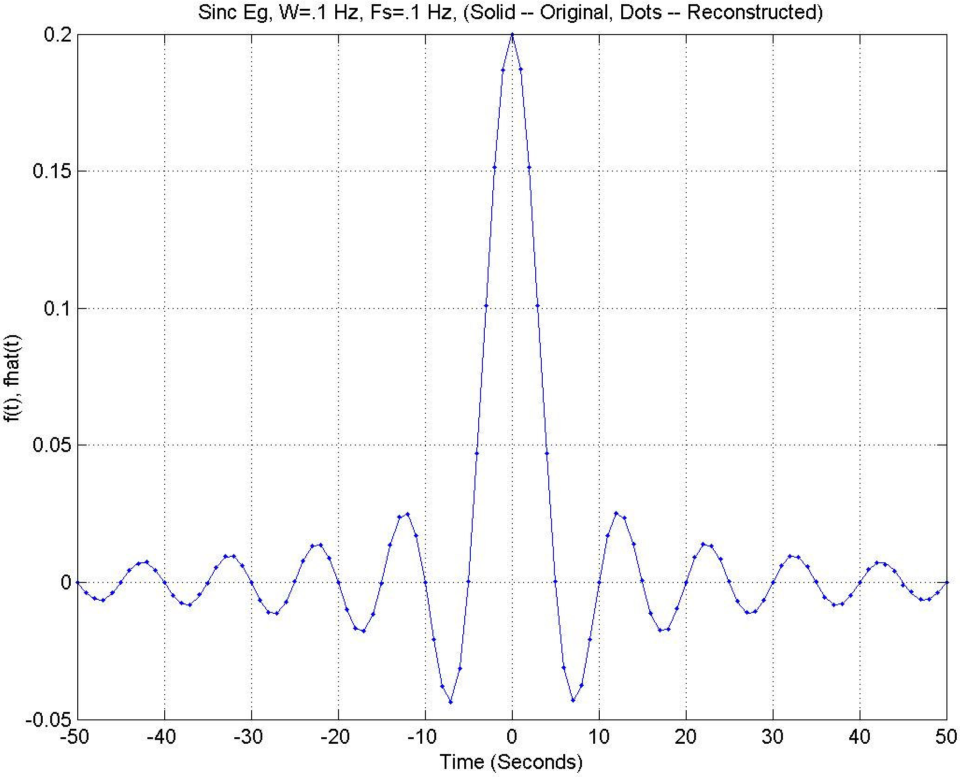

Figure 17. Reconstructed Sinc Function, 16 Bit Quantization, Tau = .05 Sec

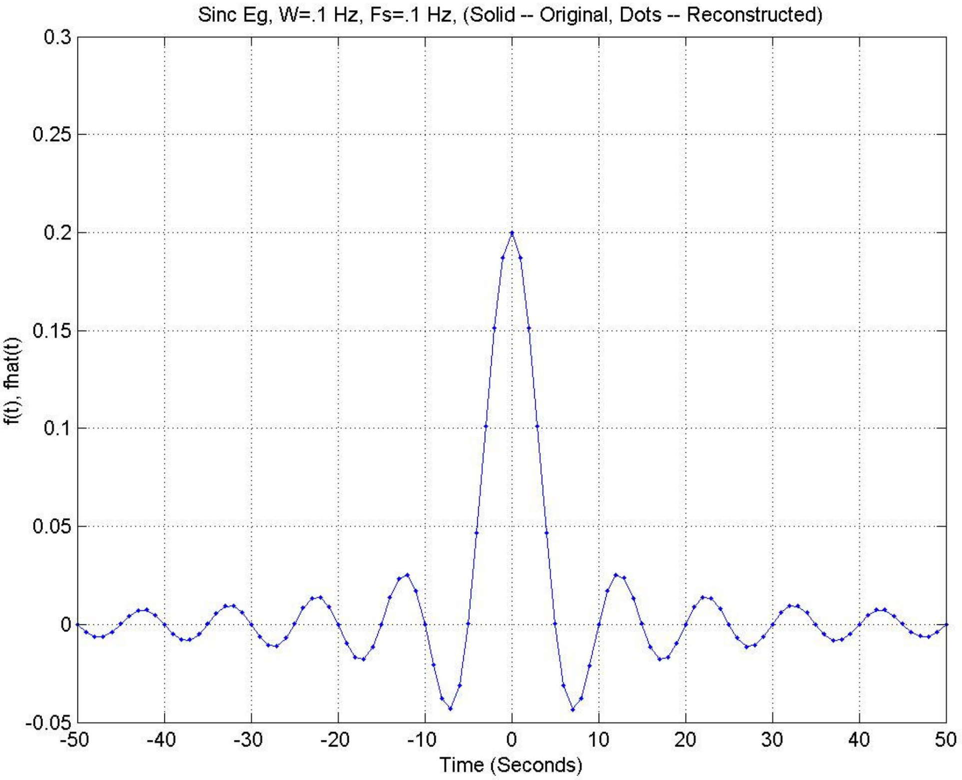

Figure 18. Reconstructed Sinc Function, 16 Bit Quantization, Tau = 1.0 Sec

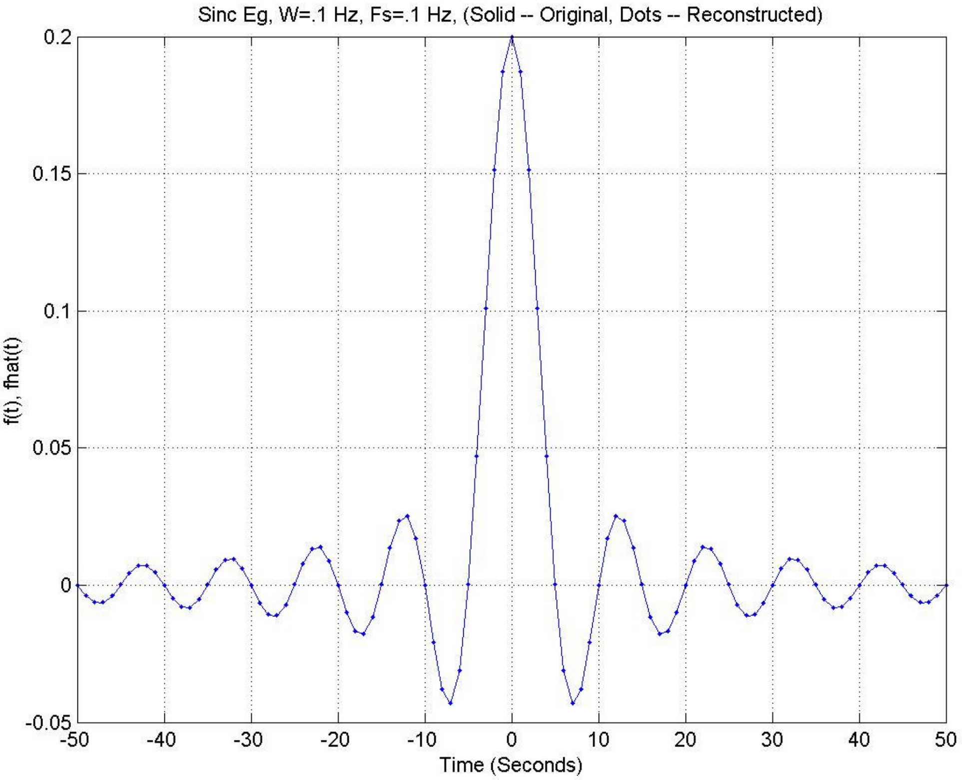

Figure 19. Reconstructed Sinc Function, 32 Bits Quantization, Tau = .001 Sec

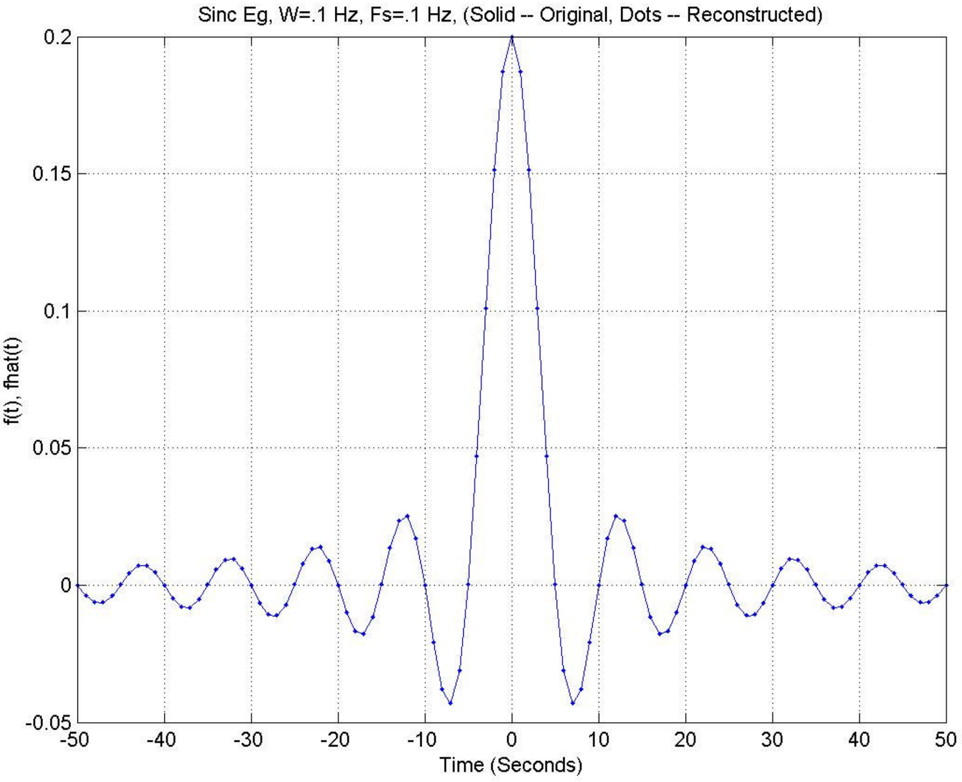

Figure 20. Reconstructed Sinc Function, 32 Bit Quantization, Tau = .005 Sec

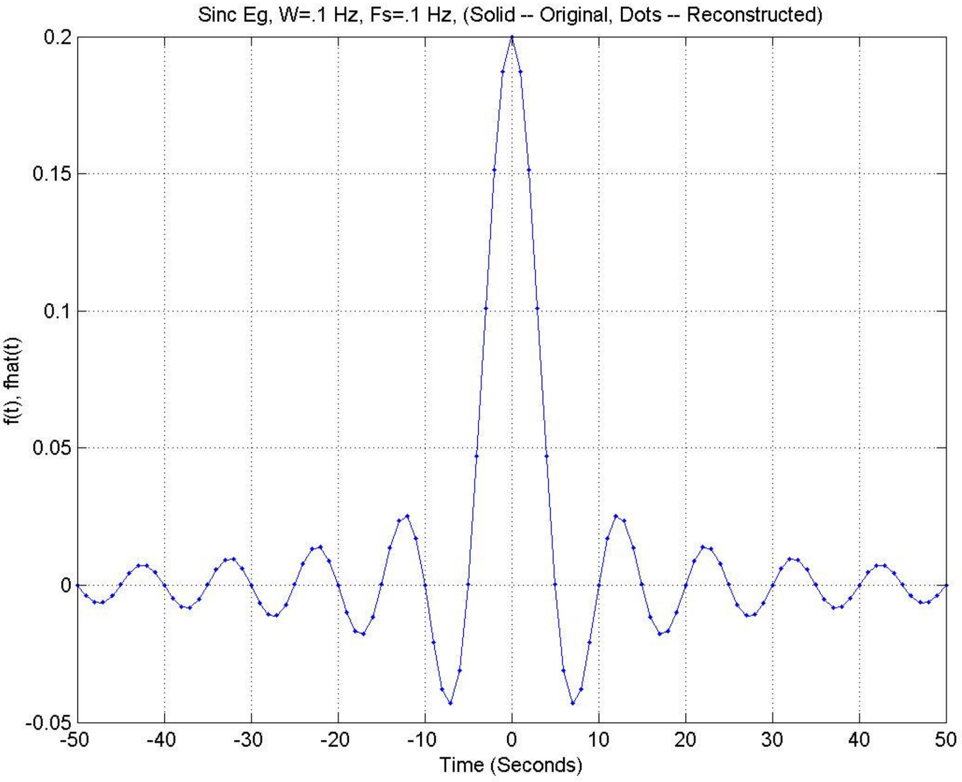

Figure 21. Reconstructed Sinc Function, 32 Bit Quantization, Tau = .01 Sec

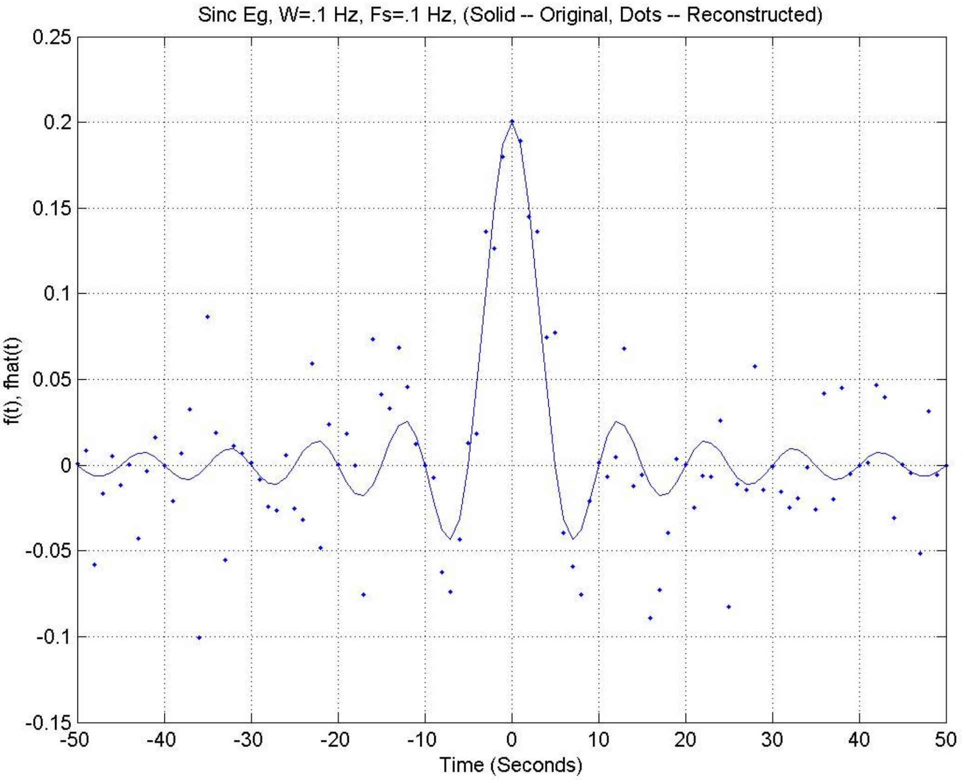

Figure 22. Reconstructed Sinc Function, 8 Bit Quantization, Tau = .05 Sec

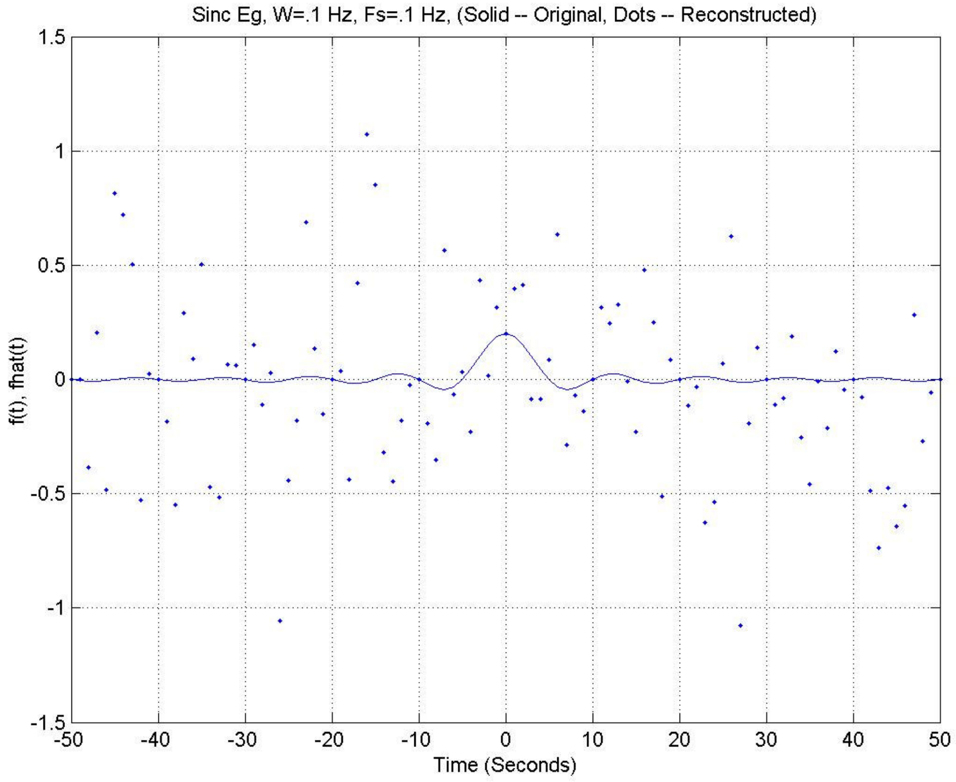

Figure 23. Reconstructed Sinc Function, 8 Bit Quantization, Tau = .01 Sec

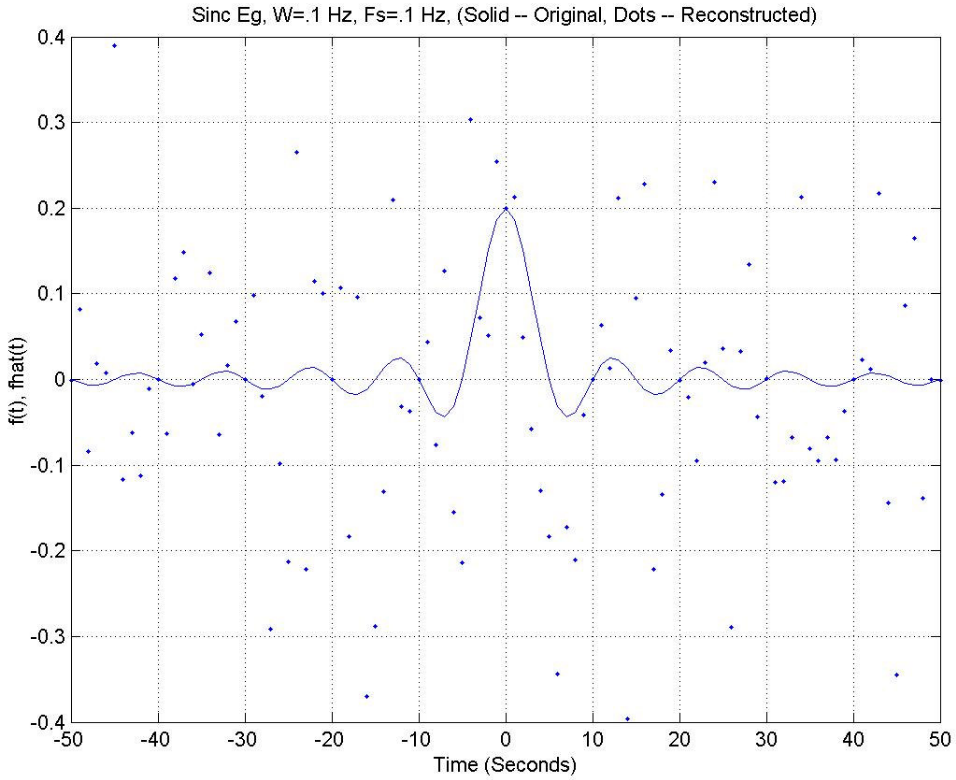

Figure 24. Reconstructed Sinc Function, 8 Bit Quantization, Tau = .025 Sec

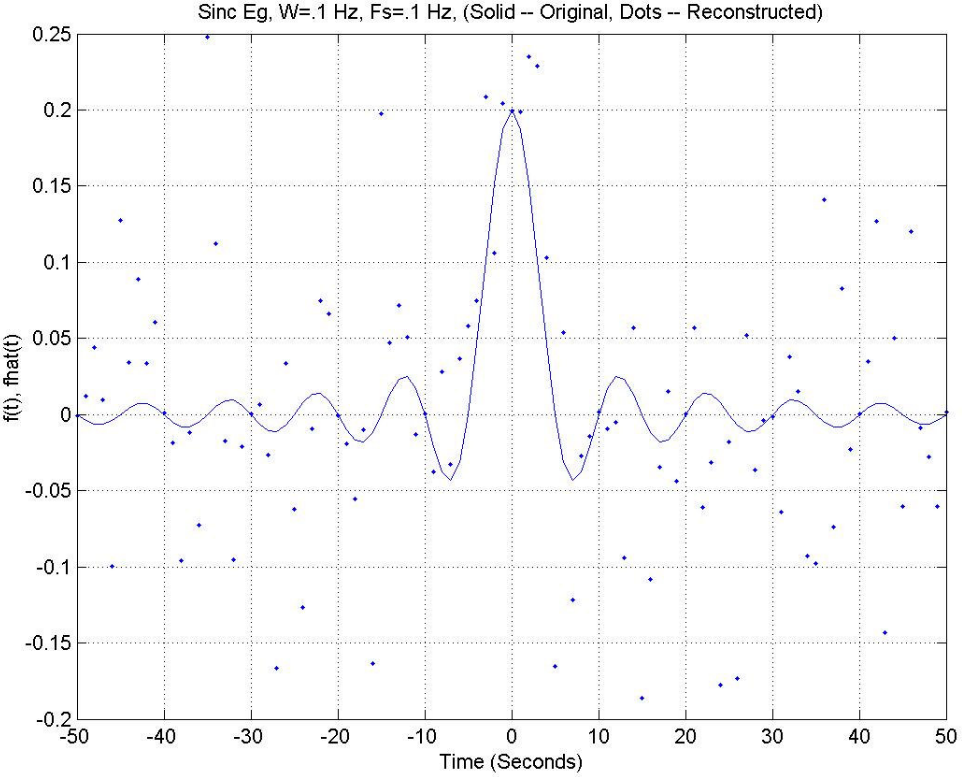

Figure 25. Reconstructed Sinc Function, 8 Bit Quantization, Tau = .05 Sec

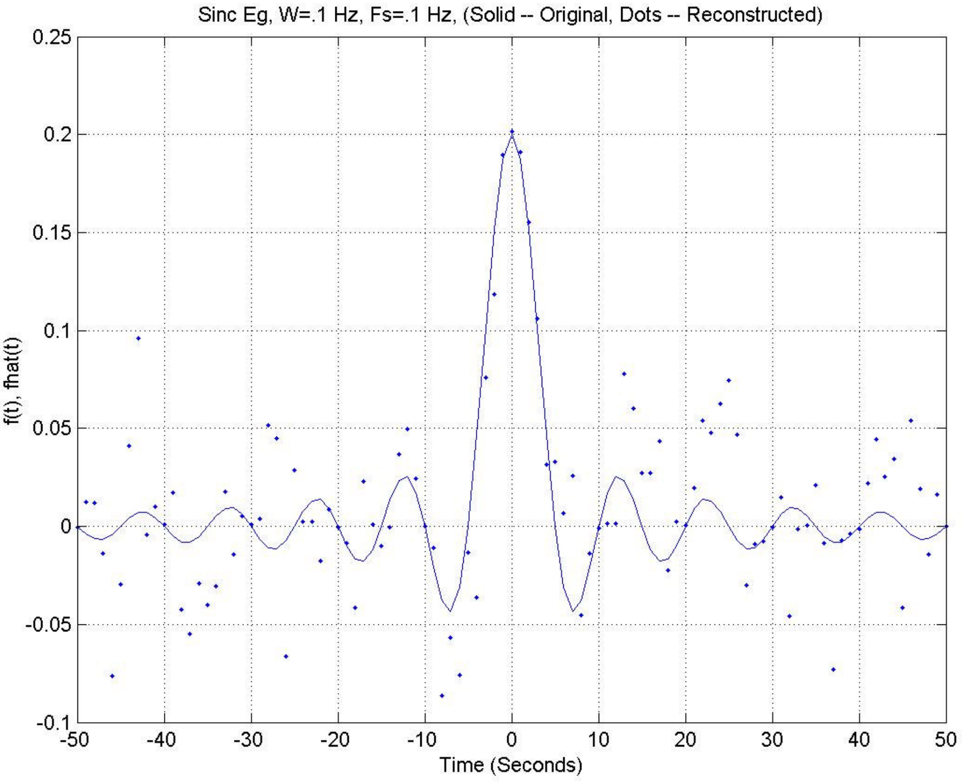

Figure 26. Reconstructed Sinc Function, 8 Bit Quantization, Tau = 1.0 Sec

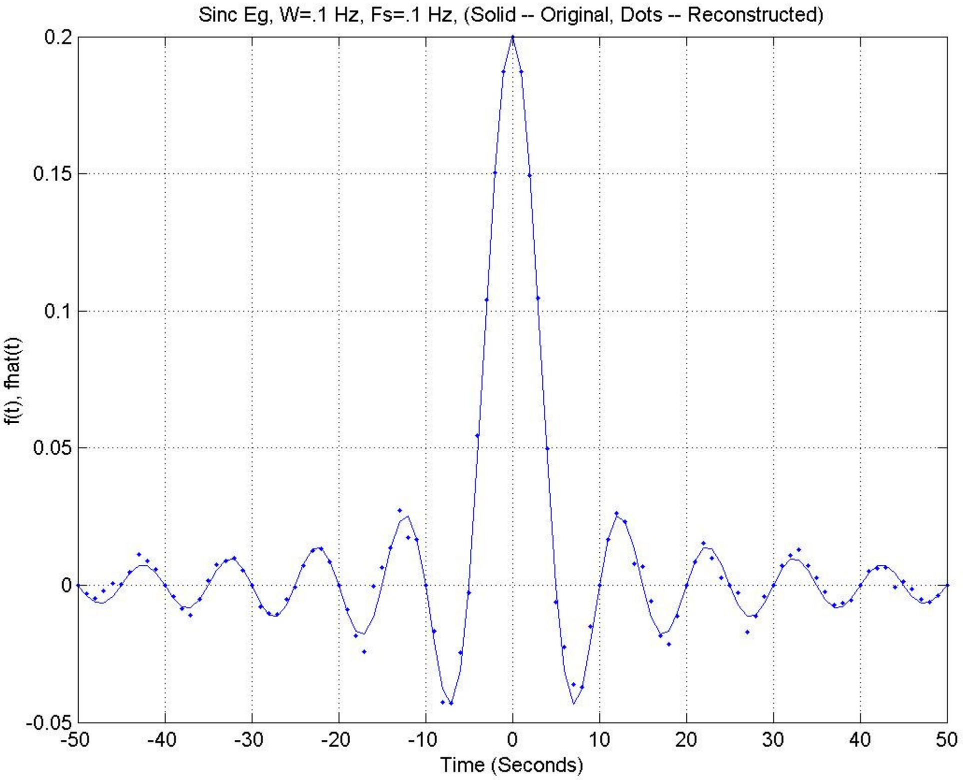

Figure 27. Reconstructed Sinc Function, Jitter Variance = .001, Tau = .01 Sec

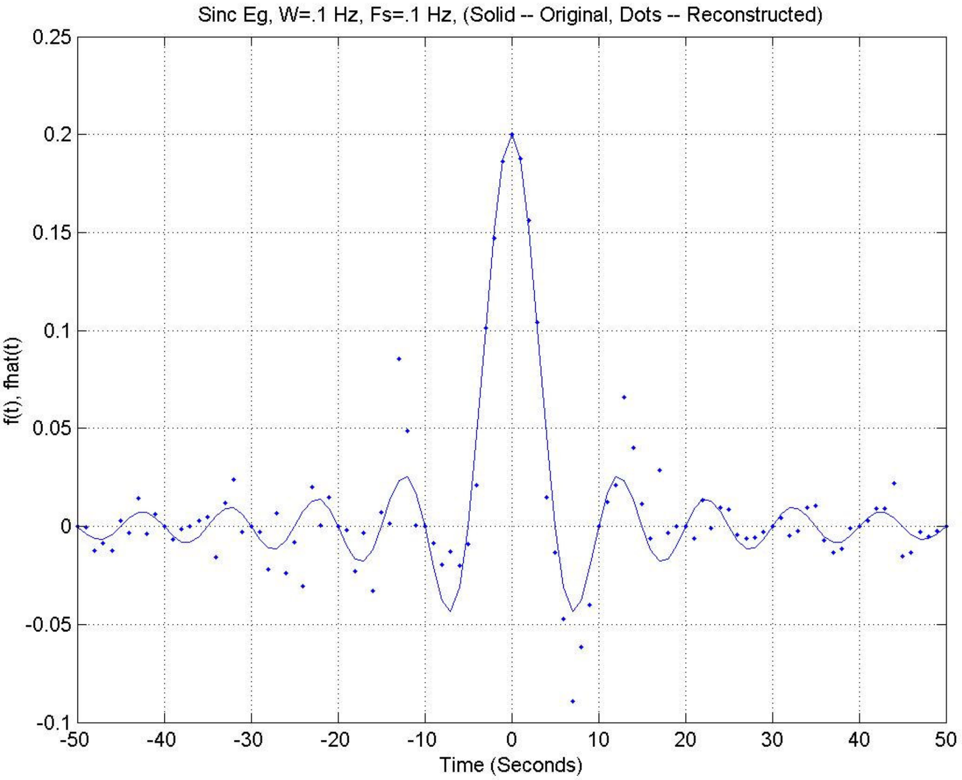

Figure 28. Reconstructed Sinc Function, Jitter Variance = .005, Tau = .01 Sec

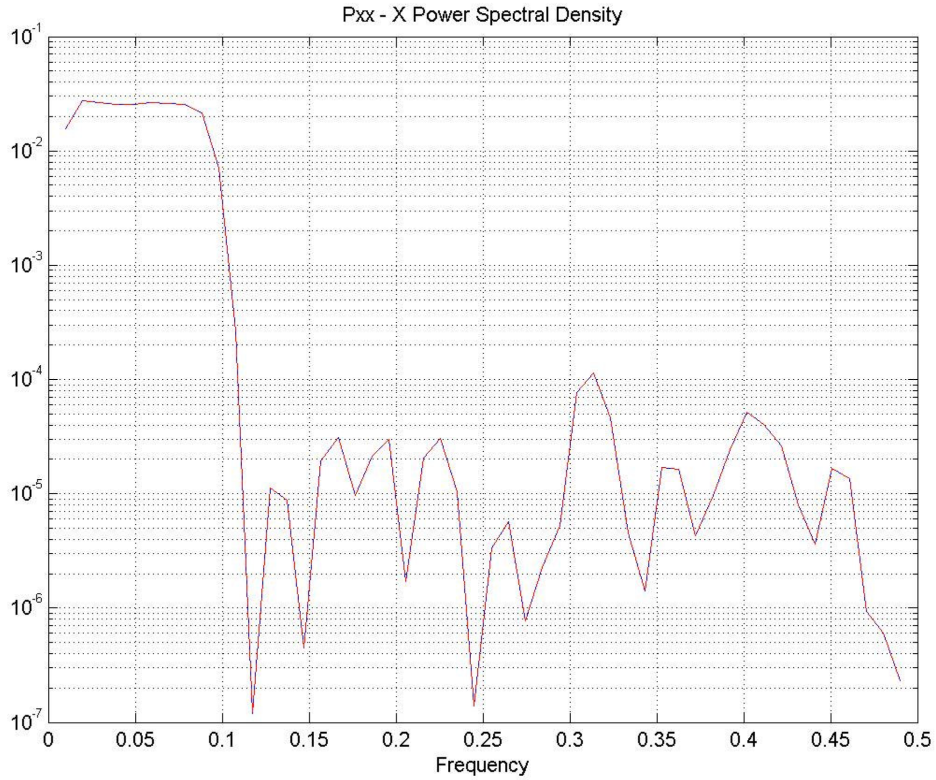

Figure 29. PSD of Sinc, Jitter Variance = .001, Tau = .01 Sec

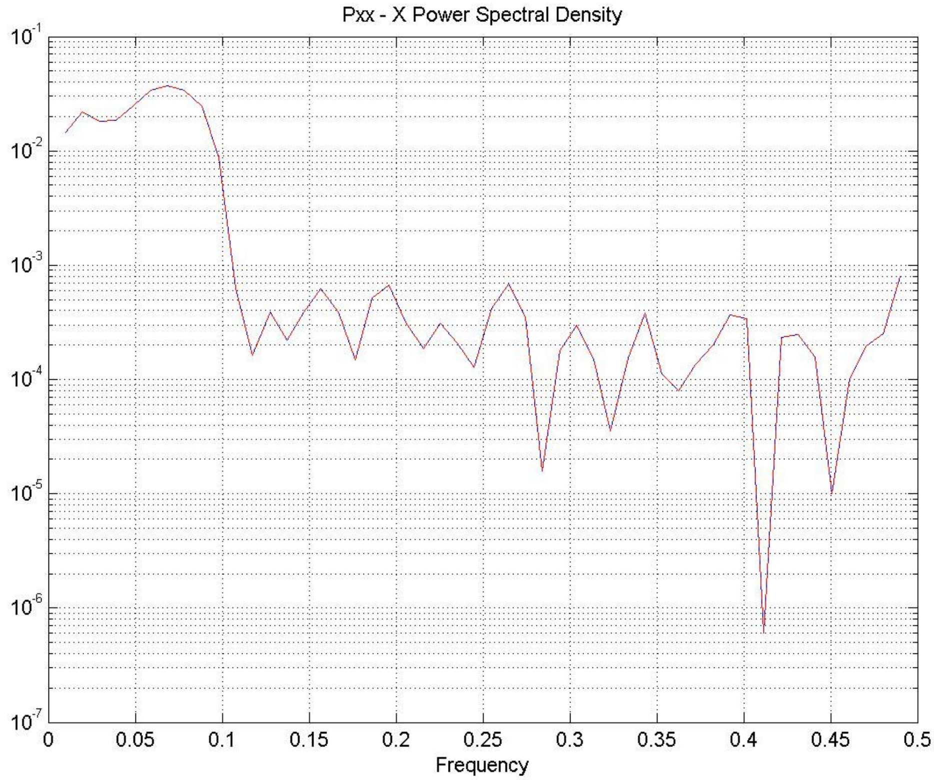

Figure 30. PSD of Sinc, Jitter Variance = .005, Tau = .01 Sec

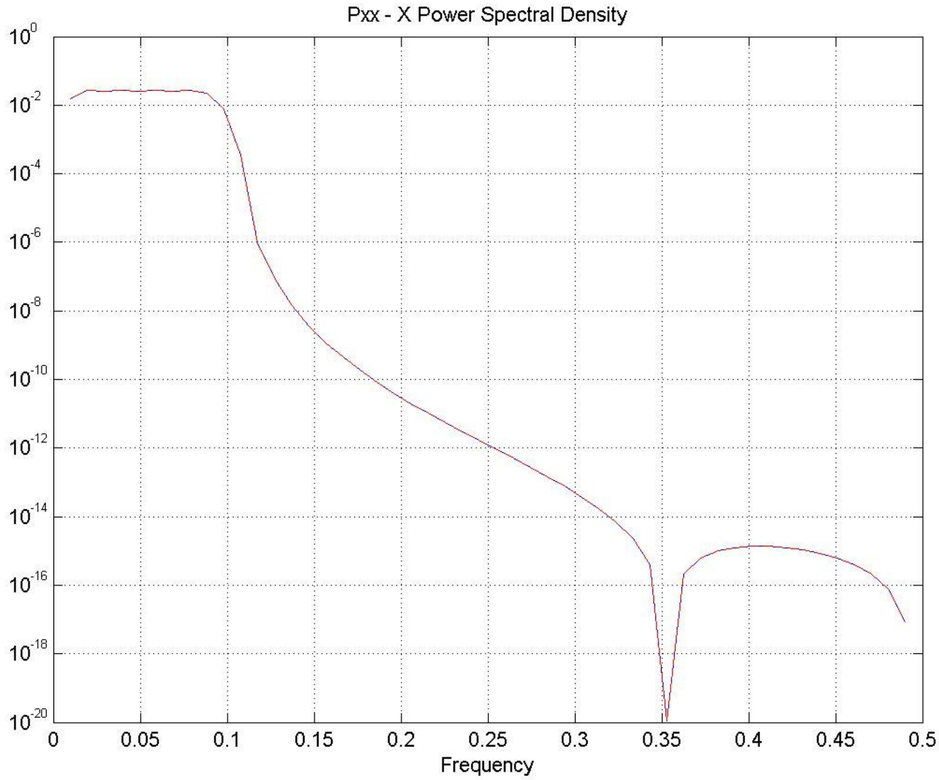

Figure 31. PSD of Sinc, No Jitter, Tau = .01 Sec

Appendix B: DASP 2004/05 Paper

Radar Waveform Design Based On the Ambiguity Function of Undersampled Signals

Jim Schroeder
University of Adelaide
DSpace Pty Ltd
Adelaide, SA 5001
schroede@eleceng.adelaide.edu.au
jim@dspace.com.au

Muralidhar Rangaswamy
AFRL/SNHE
Hanscom AFB, MA 01731
Muralidhar.Rangaswamy@hanscom.af.mil

[1]**Abstract - A primary goal in radar waveform design is to achieve a prescribed discrete time radar ambiguity function. Radar waveform design to meet a given ambiguity function specification is an important issue under the waveform diversity technology. Much of the development in this area is for continuous time signals. For the discrete time case, the sampling rate becomes an important design issue. On the one hand, too low of a sampling rate results in spectral aliasing, on the other hand, a sampling rate chosen higher than necessary increases the computational burden. We show in this paper that aliased spectra, arising from sampling below the Nyquist rate, may be completely eliminated.**

[1] The USAF AFOSR AOARD, under Contract # 044046, "Radar Waveform Design of Undersampled Signals" is supporting this research.

I. INTRODUCTION

For the purpose of this research, we assume for a start that the desired waveform is available. Since radar processing is done digitally, it is important to examine the effects of sampling the ambiguity function in the Delay-Doppler plane and study the resulting resolution trade-offs, reconstruction issues, and aliasing problems. The preliminary techniques developed in this research, and applied to the ambiguity function, should be quite useful in this context.

The approach for this research will be to apply the proposed aliased signal reconstruction algorithms to radar waveform design against ambiguity plane constraints. We hypothesise, based on simulation results, that the reconstruction algorithm is valid for bandlimited random processes.

Another component of the research is to prove analytically that exact reconstruction of bandlimited random

processes is possible in a "Limit in the Mean" sense. This is an important result since modern radar waveform design involves the use of pseudorandom coding for pulse compression and LPI/LPD waveforms.

In addition to analytically proving convergence of the reconstruction algorithm, we plan to present design trade-off plots using Matlab-based simulation tools.

The effect of A/D quantisation noise, impulse doublet spacing, and sample timing jitter, need to be quantified via simulation, before the potential use of these reconstruction algorithms can be considered for an operational radar system. Matlab-based simulation tools will be utilised to develop reconstruction sensitivities to the various real-world degradations listed above. For off-line waveform design purposes, noise sensitivities may be less of an issue.

II. APPLICATIONS TO RADAR WAVEFORM DESIGN

A primary goal in radar waveform design is to achieve a prescribed discrete time radar ambiguity function. Radar waveform design to meet a given ambiguity function specification is an important issue under the waveform diversity technology. Much of the development in this area is for continuous time signals. For the discrete time case, the sampling rate becomes an important design issue. On the one hand, too low of a sampling rate results in spectral aliasing, on the other hand, a sampling rate chosen higher than necessary increases the computational burden. We show in this research project that aliased spectra, arising from sampling below the Nyquist rate, may be completely eliminated.

The radar ambiguity function based waveform design is complicated by the fact that for a given waveform, the ambiguity function can be readily calculated. However, given an ambiguity function specification, it is possible to have more than one waveform that meets the specification. For the purpose of this research, we assume for a start that the desired waveform is available. Since radar processing is done digitally, it is important to examine the effects of sampling the ambiguity function in the Delay-Doppler plane and study the resulting resolution trade-offs, reconstruction issues, and aliasing problems. The preliminary techniques developed in this research, and applied to the ambiguity function in this proposed research, should be quite useful in this context.

The goal of this research is to apply the aliased signal reconstruction algorithm to radar waveform design against ambiguity plane constraints [19]. The radar receiver discrete time matched filter computational complexity may be potential reduced by implementing the signal restoration algorithm summarised in this proposal. We hypothesise, based on simulation results presented here, that the reconstruction algorithm is valid for bandlimited random processes.

III. SAMPLING THEORIES

Research into representing a function by its sample values, and development of the corresponding interpolation formulas, enjoys a rich history [1-11]. Representations may be chosen, e.g. by use of Fourier series coefficients, that do not restrict the frequency domain

support. Although Fourier coefficients are attractive for many reasons, a variety of interpolation functions have been invoked [1,3,4,7]. Other convenient representations, e.g. use of the function sample values directly, require the function to be bandlimited. Bandlimited functions that are sampled at less than the Nyquist rate [2] exhibit a distortion termed aliasing, however, many situations allow the aliasing to be eliminated or reduced if additional information is available at the sampling instants [8,9,11,12,15-18].

IV. IMPULSE-DOUBLET SAMPLING

A generalised version of the Nyquist sampling theorem [8] admits sampling at an average rate equal to twice the highest frequency component of the sampled signal. For example, we may envision a sampling structure wherein a pair of closely spaced impulses perform the signal sampling, each impulse pair sampling the signal at one-half the minimum rate required for ideal impulse sampling. Let f(t) be a low pass signal with bandwidth f_c = W Hz that is sampled by the function

$$p(t) = \delta(t + \tau/2) + \delta(t - \tau/2)$$

at a rate $f_s = f_c = 1/T$ Hz, $0 < \tau << T/2$. We assume that f(t) is real so that the sampled spectrum is Hermitian, and may be restored using positive frequencies only. The aliased spectrum, $F^*(\omega)$ over $0 \leq f \leq f_c$ (using $\omega = 2\pi f$ to avoid notational difficulties) is given by

$$F^*(\omega) = A_0 F(\omega) + A_1 F(\omega - \omega_s)$$

where

$$A_m = (2/T) \cos(m\omega_c\tau/2)$$

As shown in Figure 1.

V. RECONSTRUCTION EQUATIONS

We next derive a frequency domain restoration algorithm and its corresponding time domain interpolation formula. Straightforward manipulation of the aliased spectral equations results in the solution

$$F = A^{-1}F^*$$

with

$$A = \begin{bmatrix} A_0 & A_1 \\ A_1 & A_0 \end{bmatrix}$$

$$F = \begin{bmatrix} F(\omega_0 + \Delta\omega) \\ F(\omega_0 - \Delta\omega) \end{bmatrix}$$

$$F^* = \begin{bmatrix} F^*(\omega_0 + \Delta\omega) \\ F^*(\omega_0 - \Delta\omega) \end{bmatrix}$$

where $\omega_0 = \omega_c/2$, and $\Delta\omega$ is an arbitrary frequency offset from ω_0.

The interpolation equation follows directly as

$$f(t) = 2\,\mathrm{Re}\left\{ \sum_{n=-\infty}^{n=+\infty} \begin{bmatrix} x(nT + \tau/2)g(t - nT + \tau/2) \\ + x(nT - \tau/2)g(t - nT - \tau/2) \end{bmatrix} \right\}$$

with

$$g(t) = \frac{W \sin(\pi W t)}{\pi W t} e^{j\pi W t}$$

$$x(t) = \frac{A_0 - A_1 e^{j2\pi Wt}}{A_0^2 - A_1^2} f^*(t)$$

where $f^*(t)$ is the sampled version of f(t).

Finally, we quantify the effect of impulse pair spacing on the numerical conditioning of the restoration algorithm.

The eigenvalues of matrix A are A_0 +/- A_1, A_0, $A_1 > 0$; therefore the matrix Condition Number of A is given by

$$C.N. = \frac{A_0 + A_1}{A_0 - A_1}$$

$$A_0 = \frac{2}{T}$$

$$A_1 = \frac{2}{T}\cos(\pi W\tau).$$

We observe that:

- As τ approaches zero the C.N. $\rightarrow \infty$ as we expect, i.e., no reconstruction is possible

- As τ approaches T/2 the C.N. $\rightarrow$ 1, i.e., $A_1 = 0$, the aliasing is zero, and conventional ideal impulse sampling at the Nyquist rate obtains in the limit

- For $0 < \tau < T/2$ numerical stability of the time domain interpolation formula or the frequency domain alias removal algorithms are clearly a function of the impulse-doublet spacing.

VI. SIMULATION RESULTS

The following simulations illustrate that reconstruction is possible with the aliased components removed. We consider an ideal test signal, the "Sinc Function," as well as a realistic signal, Bandlimited Noise, and its ambiguity function. We also show the ambiguity function of the reconstructed sinc function.

Figure 2. shows the results of sampling a .1 Hz bandwidth "Sinc Function," at .1 Hz. We reconstruct 100 points, with each reconstructed point estimated from a 500 point summation. The impulse doublet has width .1 Second for this example. No noise has been added.

The next example illustrates that reconstruction of a random process is possible. White Gaussian Noise was filtered to .1 Hz with a 500 tap FIR filter. The sampling rate is .1 Hz. In Figure 3. we illustrate the reconstruction of this random process.

Figures 4., 5., and 6., show the equivalence of the ambiguity functions computed from the original signals or reconstructed signals from aliased copies.

VII. CONCLUSIONS

We have summarised time domain and frequency domain restoration algorithms for a signal sampled by a periodic impulse-doublet at a rate equal to one-half the conventional Nyquist rate. The numerical stability of the proposed solution is a function of the C.N. of matrix A, directly related to the impulse-doublet spacing. The problem becomes ill posed as $\tau \rightarrow 0$. We presented simulation results that demonstrate the accuracy of the time domain

reconstruction equations with and without noise. Finally, we note that there does not appear to be any mathematical reason the sampling rate cannot be reduced, and the additional aliased spectra restored in an extended solution to the simplified case we considered here of first order aliasing.

Based upon the simulation results applied to reconstructing a bandlimited random process, we postulate that the restoration equations presented here are indeed valid for bandlimited random processes. A goal of this proposed research is to prove that reconstruction of an aliased bandlimited random process is possible in a "Limit in the Mean" sense.

The effect of A/D quantisation noise, and sample timing jitter, need to be quantified via simulation, before the potential use of these reconstruction algorithms can be considered for an operational radar system. For off-line waveform design purposes, noise sensitivities may be less of an issue.

We propose to extend these results to reducing or eliminating the aliasing in an ambiguity function computed from an undersampled radar waveform. This proposed research would lead to a better understanding of the effects of sampling, and aliasing, on the ambiguity function computed from a digitised radar waveform.

ACKNOWLEDGMENTS

The authors gratefully thank Dr. Tae-Woo Park, AFOSR/AOARD, Tokyo, Japan, for his grant support of this research.

REFERENCES

[1] E.T. Whitaker, "On the functions which are represented by the expansion of interpolating theory," Proc. Roy. Soc. Edinburgh, vol. 35, pp. 181-194, 1915.

[2] H. Nyquist, "Certain topics in telegraph transmission theory," AIEE Trans., vol. 47, pp.617-644, 1928.

[3] J.M. Whitaker, "The Fourier theory of cardinal functions," Proc. Math Soc. Edinburgh, vol. 1, pp. 169-176, 1929.

[4] D. Gabor, "Theory of communications," J. Inst. Elec. Eng. Vol. 93, no. 3, pp. 429-457, 1946.

[5] C.E. Shannon, "Communications in the presence of noise," Proc. IRE., vol. 37, pp. 10-21, Jan. 1949.

[6] H.S. Black, Modulation Theory, New York: van Nostrand, 1953.

[7] J. Zak, "Finite translations in solid-state physics," Phys. Rev. Lett., vol. 19, pp. 1385-1387, 1967.

[8] A. Papoulis, Systems and transforms with applications in optics, New York: McGraw Hill, 1968.

[9] J.M. Wozencraft and I.M. Jacobs, "Principles of communication engineering, New York: Wiley, 1965.

[10] A.J. Jerri, “The Shannon sampling theorem – Its various extensions and applications: A tutorial review,” Proc. IEEE, vol. 65, no. 11, pp. 1565-1598, November, 1977.

[11] A. Nathan, “On sampling a function and its derivatives,” Information and Control, Academic Press, vol. 22, pp. 172-182, 1973.

[12] R.J. Marks, “Restoration of a continuously sampled band-limited signal from aliased data,” IEEE ASSP, vol. ASSP-30, no. 5, pp. 937-942, December 1982.

[13] K.F. Cheung, and R.J. Marks, “Ill-posed sampling theorems,” IEEE Trans. Ckts. Sys., vol. CAS-32, no.5, May 1985.

[14] X-G Xia, and Z. Zhang, “On sampling theorem, wavelets, and wavelet transforms,” IEEE Trans. SP, vol. 41, no. 12., December 1993.

[15] P.E. Pace, R.E. Leino, and D. Styer, “Use of the symmetrical number system in resolving single-frequency undersampling aliases,” IEEE Trans. SP, vol. 45, no. 5, pp. 1153-1160, May 1997.

[16] D. Seidner, and M. Feder, “Noise amplification of periodic nonuniform sampling,” IEEE Trans. SP, vol. 48, no. 1, pp. 275-277, January 2000.

[17] M.B. Matthews, “On the linear minimum-mean-squared-error estimation of an undersampled wide-sense stationary random process,” IEEE Trans. SP, vol. 48, no. 1, pp. 272-275, January 2000.

[18] J. Angeby, “Aliasing of polynomial-phase signals,” IEEE Trans. SP, vol. 48, no. 5, pp. 1488-1491, May 2000.

[19] M.I. Skolnik, “Introduction to Radar Systems,” McGraw-Hill, New York, 1980.

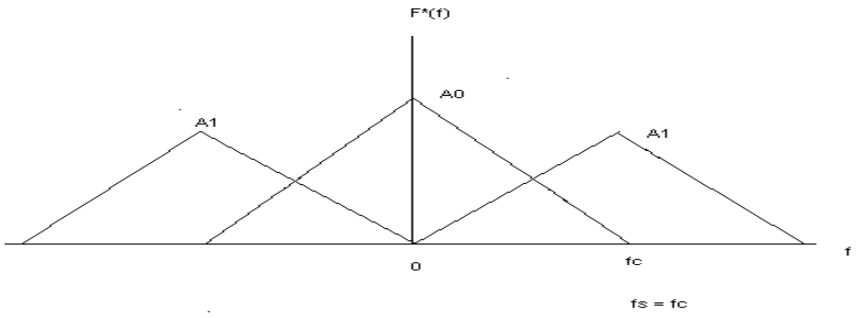

Fig. 1. Aliased Spectrum Sampled at One-Half the Nyquist Rate

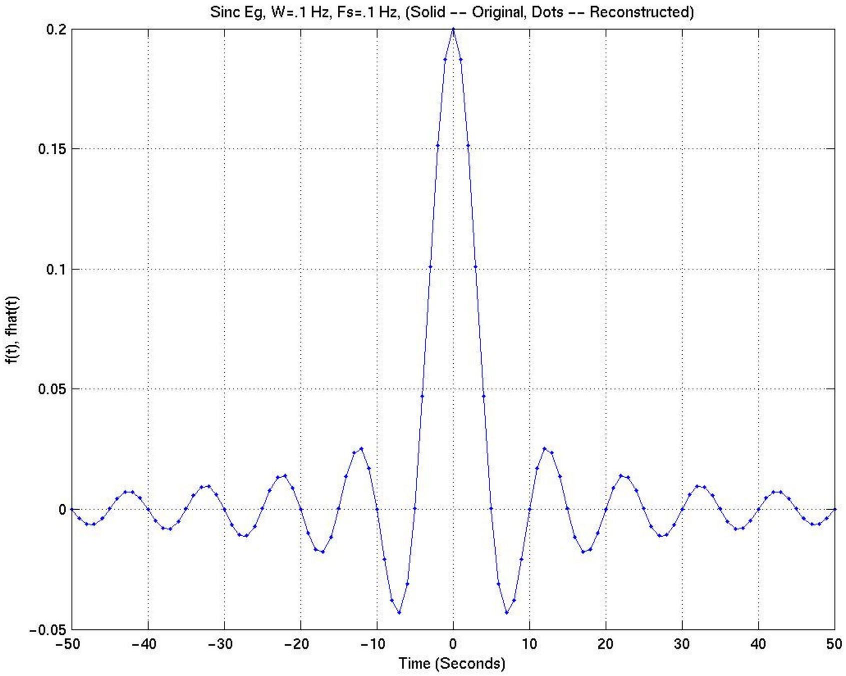

Fig. 2. Reconstructed “Sinc Function,” 500 Samples Used, τ = .01 Sec, No Added Noise

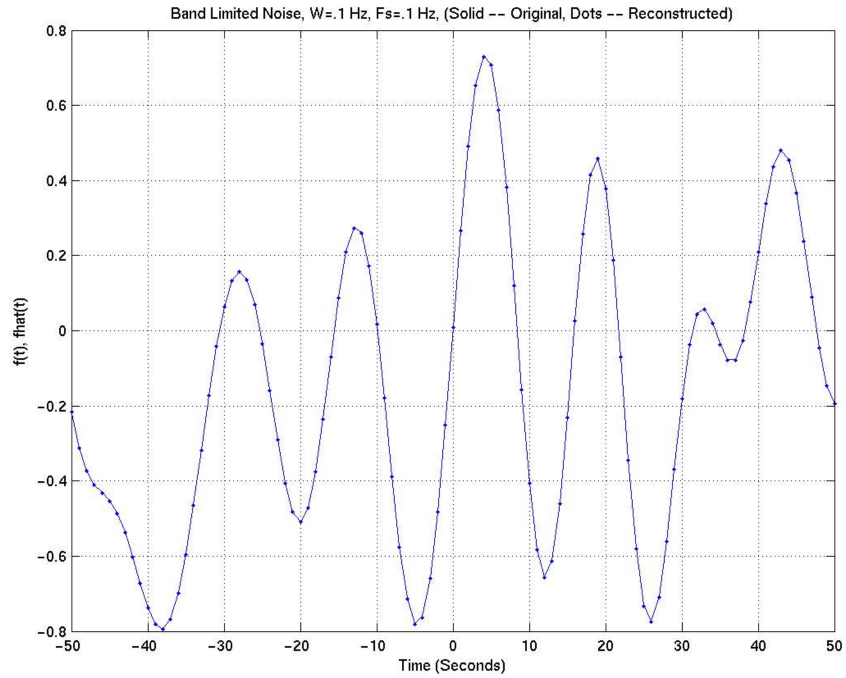

Fig. 3. Reconstructed Bandlimited Noise, τ = .01 Second

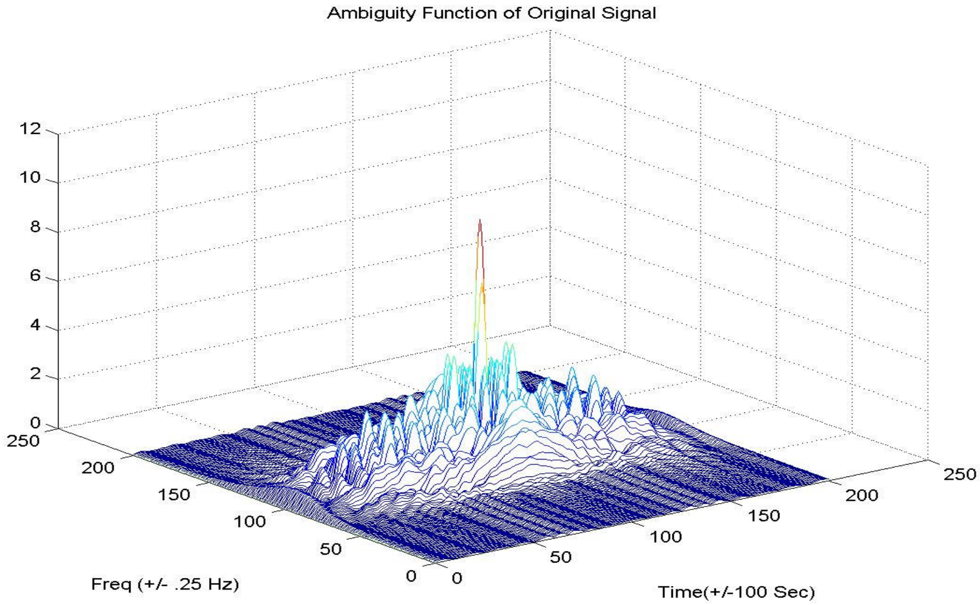

Fig. 4. Ambiguity Function of Original Signal (.1 Hz Bandlimited Noise)

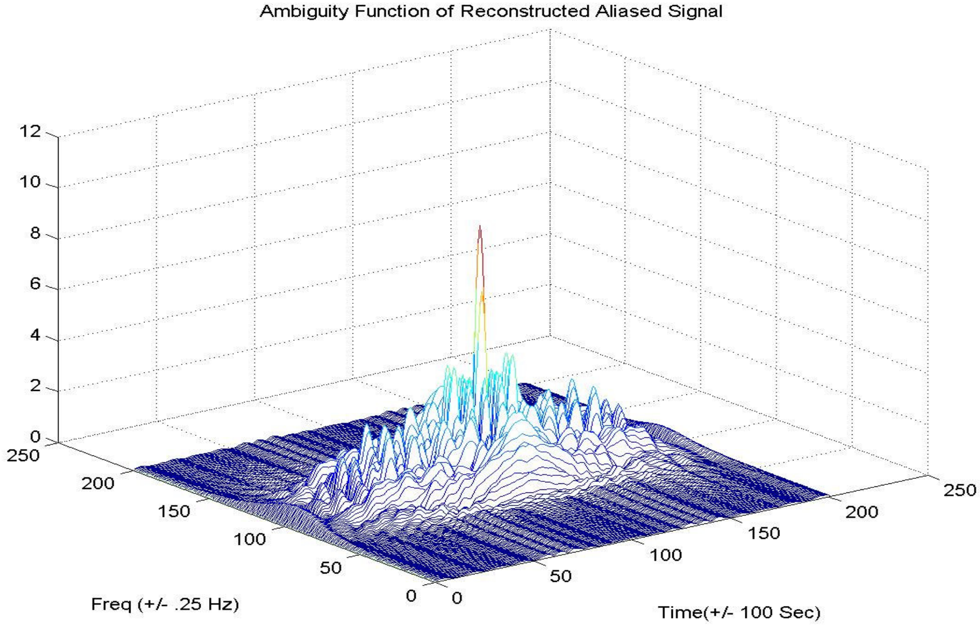

Fig. 5. Ambiguity Function of Reconstructed Signal (.1 Hz Bandlimited Noise)

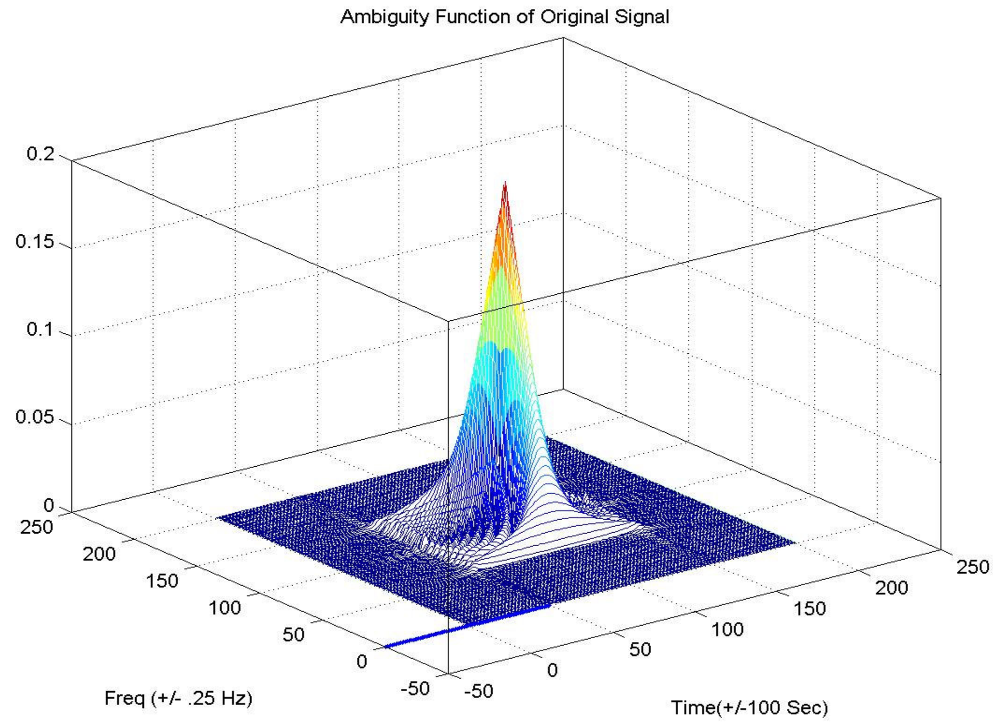

Fig. 6. Ambiguity Function of the "Sinc" Function

Appendix C: Matlab Code

```
% Reconstruction of 1/2 Nyquist Rate Sampled Signal
% Test Signal is the .25 SQRTCOS filtered 16-QAM
% BW = .2 Hz, Sampled at .2 Hz

clf
clear

Fs=1
N=4097
W=input('Enter W: ')
T=fix(1/W)
%tau=input('Enter tau: ')
tau=2
noise_var=input('Enter noise variance: ')
white_noise=sqrt(noise_var)*randn(1,N);

A0 = 2/T
A1 = (2/T)*cos(pi*W*tau)
t=-50:50;


load -MAT snr_inf.bak
qam_sig=zeros(1,N);
qam_sig(2049-1250:2049+1250)=real(MatrixData(100:2600));
w=hamming(1,2501);
%qam_sig(2049-1250:2049+1250)=w.*qam_sig(2049-1250:2049+1250);

f=zeros(1,N);
xterm1=zeros(1,N);
xterm2=zeros(1,N);
gterm1=zeros(1,N);
gterm2=zeros(1,N);

f = qam_sig + white_noise;

% Construct interpolation functions sampled at 1 Hz

for n=1:Fs:2048

  xterm1(n)=(A0-A1*exp(j*2*pi*W*(n-2049)))*f(n)/(A0^2-A1^2);
  xterm2(n)=(A0-A1*exp(j*2*pi*W*(n-2049)))*f(n)/(A0^2-A1^2);
  gterm1(n)=W*sin(pi*W*(2049-n))*exp(j*pi*W*(2049-n))/(pi*W*(2049-n));
  gterm2(n)=W*sin(pi*W*(2049-n))*exp(j*pi*W*(2049-n))/(pi*W*(2049-n));
```

```
end

for n=2050:Fs:4097

  xterm1(n)=(A0-A1*exp(j*2*pi*W*(n-2049)))*f(n)/(A0^2-A1^2);
  xterm2(n)=(A0-A1*exp(j*2*pi*W*(n-2049)))*f(n)/(A0^2-A1^2);
  gterm1(n)=W*sin(pi*W*(2049-n))*exp(j*pi*W*(2049-n))/(pi*W*(2049-n));
  gterm2(n)=W*sin(pi*W*(2049-n))*exp(j*pi*W*(2049-n))/(pi*W*(2049-n));

end



xterm1(2049)=(A0-A1)*f(2049)/(A0^2-A1^2);
xterm2(2049)=(A0-A1)*f(2049)/(A0^2-A1^2);
gterm1(2049)=W;
gterm2(2049)=W;



%Interpolate at .2 Hz sampling

f_hat_save=zeros(1,length(t));

for t_index=1:length(t)

    f_hat=zeros(1,length(t));

%for m = T+length(t)+1:T:N-T-length(t)

count=0;

for m = 2049-1250:T:2049+1250

count=count+1;

m_save(count)=m;

  f_hat(t_index) = f_hat(t_index) + xterm1(m+tau/2)*gterm1(-t(t_index)+m+tau/2) +
xterm2(m-tau/2)*gterm2(-t(t_index)+m-tau/2);

end

f_hat_save(t_index)=2*real(f_hat(t_index));

end
```

```
f_test=f(2049-fix(length(t)/2):2049+fix(length(t)/2))

f_hat_save

snr=10*log10(sum(qam_sig.^2)/noise_var)
mse=sum((f_test-f_hat_save).^2)

y=2*W*real(conv(xterm1,gterm1) + conv(xterm2,gterm2));
y(4097-fix(length(t)/2):4097+fix(length(t)/2))

plot(t,f_test)
hold on
plot(t,f_hat_save,'.')
grid
xlabel('Time (Seconds)')
ylabel('f(t), fhat(t)')
title('16-QAM Eg, W=.2 Hz, Fs=.2 Hz, (Solid -- Original, Dots -- Reconstructed)')
```

```
% Reconstruction of 1/2 Nyquist Rate Sampled Signal
% Test Signal is the Sinc function
% BW = .1 Hz, Sampled at .1 Hz


Fs=.1
N=500
Fc=.1
W=.1
T=1/W
tau=input('Enter tau: ')
noise_var=input('Enter noise variance: ')
A0 = 2/T
A1 = (2/T)*cos(pi*W*tau)
t=-50:50

for t_index=1:length(t)
t_index

f=zeros(2,N);
xterm1=zeros(1,N);
xterm2=zeros(1,N);
gterm1=zeros(1,N);
gterm2=zeros(1,N);


% Construct test signal and interpolation functions sampled at 1 Hz

for n=1:N

arg=(n-N/2)*T;

  f(1,n) = 2*W*sin(2*pi*W*(arg+tau/2))/(2*pi*W*(arg+tau/2)) +
sqrt(noise_var)*randn(1,1);
  f(2,n) = 2*W*sin(2*pi*W*(arg-tau/2))/(2*pi*W*(arg-tau/2)) +
sqrt(noise_var)*randn(1,1);

  xterm1(n)=(A0-A1*exp(j*2*pi*W*(arg+tau/2)))*f(1,n)/(A0^2-A1^2);
  xterm2(n)=(A0-A1*exp(j*2*pi*W*(arg-tau/2)))*f(2,n)/(A0^2-A1^2);
  gterm1(n)=W*sin(pi*W*(t(t_index)-arg-tau/2))*exp(j*pi*W*(t(t_index)-arg-
tau/2))/(pi*W*(t(t_index)-arg-tau/2));
  gterm2(n)=W*sin(pi*W*(t(t_index)-arg+tau/2))*exp(j*pi*W*(t(t_index)-
arg+tau/2))/(pi*W*(t(t_index)-arg+tau/2));

end
```

```
%for n=(N/2)+1:N

%  arg=(n-249)*T;

%  f(1,n) = 2*W*sin(2*pi*W*(arg+tau/2))/(2*pi*W*(arg+tau/2));
%  f(2,n) = 2*W*sin(2*pi*W*(arg-tau/2))/(2*pi*W*(arg-tau/2));

%  xterm1(n)=(A0-A1*exp(j*2*pi*W*(arg+tau/2)))*f(1,n)/(A0^2-A1^2);
%  xterm2(n)=(A0-A1*exp(j*2*pi*W*(arg-tau/2)))*f(2,n)/(A0^2-A1^2);
%  gterm1(n)=W*sin(pi*W*(-arg+tau/2))*exp(j*pi*W*(-arg+tau/2))/(pi*W*(-
arg+tau/2));
%  gterm2(n)=W*sin(pi*W*(-arg-tau/2))*exp(j*pi*W*(-arg-tau/2))/(pi*W*(-arg-tau/2));

%end


%f(N/2) = 2*W;
%xterm1(N/2)=(A0-A1)*f(N/2)/(A0^2-A1^2);
%xterm2(N/2)=(A0-A1)*f(N/2)/(A0^2-A1^2);
%gterm1(N/2)=W;
%gterm2(N/2)=W;



% Interpolate at .1 Hz sampling

f_hat_0=0;

for m=1:N

  f_hat_0 = f_hat_0 + xterm1(m)*gterm1(m) + xterm2(m)*gterm2(m);

end

f_hat_0_save(t_index)=2*real(f_hat_0);

%2*real(f_hat_0)

%f(1,N/2)
%f(2,N/2)

end

f_test=zeros(1,length(t));

for n=1:50
```

```
 f_test(n) = 2*W*sin(2*pi*W*t(n))/(2*pi*W*t(n));
 f_test(n+51) = 2*W*sin(2*pi*W*t(n+51))/(2*pi*W*t(n+51));
end

f_test(51)=.2;

plot(t,f_test)
hold on
plot(t,f_hat_0_save,'.')
grid
xlabel('Time (Seconds)')
ylabel('f(t), fhat(t)')
title('Sinc Eg, W=.1 Hz, Fs=.1 Hz, (Solid -- Original, Dots -- Reconstructed)')
```

```
% Reconstruction of 1/2 Nyquist Rate Sampled Signal
% Test Signal is the Sinc function
% BW = .1 Hz, Sampled at .1 Hz


Fs=.1
N=500
Fc=.1
W=.1
T=1/W
tau=input('Enter tau: ')
noise_var=input('Enter noise variance: ')
A0 = 2/T
A1 = (2/T)*cos(pi*W*tau)
t=-50:50

for t_index=1:length(t)
t_index

f=zeros(2,N);
xterm1=zeros(1,N);
xterm2=zeros(1,N);
gterm1=zeros(1,N);
gterm2=zeros(1,N);


% Construct test signal and interpolation functions sampled at 1 Hz

for n=1:N

arg=(n-N/2)*T;

  f(1,n) = 2*W*sin(2*pi*W*(arg+tau/2))/(2*pi*W*(arg+tau/2)) +
sqrt(noise_var)*randn(1,1);
  f(2,n) = 2*W*sin(2*pi*W*(arg-tau/2))/(2*pi*W*(arg-tau/2)) +
sqrt(noise_var)*randn(1,1);

  xterm1(n)=(A0-A1*exp(j*2*pi*W*(arg+tau/2)))*f(1,n)/(A0^2-A1^2);
  xterm2(n)=(A0-A1*exp(j*2*pi*W*(arg-tau/2)))*f(2,n)/(A0^2-A1^2);
  gterm1(n)=W*sin(pi*W*(t(t_index)-arg-tau/2))*exp(j*pi*W*(t(t_index)-arg-
tau/2))/(pi*W*(t(t_index)-arg-tau/2));
  gterm2(n)=W*sin(pi*W*(t(t_index)-arg+tau/2))*exp(j*pi*W*(t(t_index)-
arg+tau/2))/(pi*W*(t(t_index)-arg+tau/2));

end
```

```
%for n=(N/2)+1:N

%  arg=(n-249)*T;

%  f(1,n) = 2*W*sin(2*pi*W*(arg+tau/2))/(2*pi*W*(arg+tau/2));
%  f(2,n) = 2*W*sin(2*pi*W*(arg-tau/2))/(2*pi*W*(arg-tau/2));

%  xterm1(n)=(A0-A1*exp(j*2*pi*W*(arg+tau/2)))*f(1,n)/(A0^2-A1^2);
%  xterm2(n)=(A0-A1*exp(j*2*pi*W*(arg-tau/2)))*f(2,n)/(A0^2-A1^2);
%  gterm1(n)=W*sin(pi*W*(-arg+tau/2))*exp(j*pi*W*(-arg+tau/2))/(pi*W*(-
arg+tau/2));
%  gterm2(n)=W*sin(pi*W*(-arg-tau/2))*exp(j*pi*W*(-arg-tau/2))/(pi*W*(-arg-tau/2));

%end


%f(N/2) = 2*W;
%xterm1(N/2)=(A0-A1)*f(N/2)/(A0^2-A1^2);
%xterm2(N/2)=(A0-A1)*f(N/2)/(A0^2-A1^2);
%gterm1(N/2)=W;
%gterm2(N/2)=W;



% Interpolate at .1 Hz sampling

f_hat_0=0;

for m=1:N

  f_hat_0 = f_hat_0 + xterm1(m)*gterm1(m) + xterm2(m)*gterm2(m);

end

f_hat_0_save(t_index)=2*real(f_hat_0);

%2*real(f_hat_0)

%f(1,N/2)
%f(2,N/2)

end

f_test=zeros(1,length(t));

for n=1:50
```

```
 f_test(n) = 2*W*sin(2*pi*W*t(n))/(2*pi*W*t(n));
 f_test(n+51) = 2*W*sin(2*pi*W*t(n+51))/(2*pi*W*t(n+51));
end

f_test(51)=.2;

plot(t,f_test)
hold on
plot(t,f_hat_0_save,'.')
grid
xlabel('Time (Seconds)')
ylabel('f(t), fhat(t)')
title('Sinc Eg, W=.1 Hz, Fs=.1 Hz, (Solid -- Original, Dots -- Reconstructed)')

figure(2)
amb_test=ambiguity(f_test,'true');
waterfall(amb_test)
xlabel('Time(+/-100 Sec)')
ylabel('Freq (+/- .25 Hz)')
title('Ambiguity Function of Original Signal')

figure(3)
amb_test_hat=ambiguity(f_hat_0_save,'true');
waterfall(amb_test_hat)
xlabel('Time(+/-100 Sec)')
ylabel('Freq (+/- .25 Hz)')
title('Ambiguity Function of Reconstructed Signal')
```

```
% Reconstruction of 1/2 Nyquist Rate Sampled Signal
% Test Signal is the Sinc function with JITTER on sampling
% BW = .1 Hz, Sampled at .1 Hz


Fs=.1
N=500
Fc=.1
W=.1
T=1/W
tau=input('Enter tau: ')
noise_var=input('Enter noise variance: ')
%b=input('Enter number of bits: ')
%delta=2^-b;
A0 = 2/T
A1 = (2/T)*cos(pi*W*tau)
t=-50:50

for t_index=1:length(t)
t_index

f=zeros(2,N);
xterm1=zeros(1,N);
xterm2=zeros(1,N);
gterm1=zeros(1,N);
gterm2=zeros(1,N);


% Construct test signal and interpolation functions sampled at 1 Hz

for n=1:N

arg=(n-N/2)*T;

  jit1=noise_var*randn(1,1);
  jit2=noise_var*randn(1,1);

  f(1,n) = 2*W*sin(2*pi*W*(arg+tau/2 + jit1))/(2*pi*W*(arg+tau/2 + jit1));
  f(2,n) = 2*W*sin(2*pi*W*(arg-tau/2 + jit2))/(2*pi*W*(arg-tau/2 + jit2));

  xterm1(n)=(A0-A1*exp(j*2*pi*W*(arg+tau/2)))*f(1,n)/(A0^2-A1^2);
  xterm2(n)=(A0-A1*exp(j*2*pi*W*(arg-tau/2)))*f(2,n)/(A0^2-A1^2);
  gterm1(n)=W*sin(pi*W*(t(t_index)-arg-tau/2))*exp(j*pi*W*(t(t_index)-arg-
tau/2))/(pi*W*(t(t_index)-arg-tau/2));
  gterm2(n)=W*sin(pi*W*(t(t_index)-arg+tau/2))*exp(j*pi*W*(t(t_index)-
arg+tau/2))/(pi*W*(t(t_index)-arg+tau/2));
```

```
end

%for n=(N/2)+1:N

%  arg=(n-249)*T;

%  f(1,n) = 2*W*sin(2*pi*W*(arg+tau/2))/(2*pi*W*(arg+tau/2));
%  f(2,n) = 2*W*sin(2*pi*W*(arg-tau/2))/(2*pi*W*(arg-tau/2));

%  xterm1(n)=(A0-A1*exp(j*2*pi*W*(arg+tau/2)))*f(1,n)/(A0^2-A1^2);
%  xterm2(n)=(A0-A1*exp(j*2*pi*W*(arg-tau/2)))*f(2,n)/(A0^2-A1^2);
%  gterm1(n)=W*sin(pi*W*(-arg+tau/2))*exp(j*pi*W*(-arg+tau/2))/(pi*W*(-
arg+tau/2));
%  gterm2(n)=W*sin(pi*W*(-arg-tau/2))*exp(j*pi*W*(-arg-tau/2))/(pi*W*(-arg-tau/2));

%end


%f(N/2) = 2*W;
%xterm1(N/2)=(A0-A1)*f(N/2)/(A0^2-A1^2);
%xterm2(N/2)=(A0-A1)*f(N/2)/(A0^2-A1^2);
%gterm1(N/2)=W;
%gterm2(N/2)=W;



% Interpolate at .1 Hz sampling

f_hat_0=0;

for m=1:N

  f_hat_0 = f_hat_0 + xterm1(m)*gterm1(m) + xterm2(m)*gterm2(m);

end

f_hat_0_save(t_index)=2*real(f_hat_0);

%2*real(f_hat_0)

%f(1,N/2)
%f(2,N/2)

end
```

```
f_test=zeros(1,length(t));

for n=1:50
 f_test(n) = 2*W*sin(2*pi*W*t(n))/(2*pi*W*t(n));
 f_test(n+51) = 2*W*sin(2*pi*W*t(n+51))/(2*pi*W*t(n+51));
end

f_test(51)=.2;

figure(1)
plot(t,f_test)
hold on
plot(t,f_hat_0_save(1:101),'.')
grid
xlabel('Time (Seconds)')
ylabel('f(t), fhat(t)')
title('Sinc Eg, W=.1 Hz, Fs=.1 Hz, (Solid -- Original, Dots -- Reconstructed)')
hold off

figure(2)
amb_test=ambiguity(f_test,'true');
waterfall(amb_test)
xlabel('Time(+/-100 Sec)')
ylabel('Freq (+/- .25 Hz)')
title('Ambiguity Function of Original Signal')

figure(3)
amb_test_hat=ambiguity(f_hat_0_save,'true');
waterfall(amb_test_hat)
xlabel('Time(+/-100 Sec)')
ylabel('Freq (+/- .25 Hz)')
title('Ambiguity Function of Reconstructed Signal')
```

```
% Reconstruction of 1/2 Nyquist Rate Sampled Signal
% Test Signal is the Sine function
% BW = .1 Hz, Sampled at .1 Hz


Fs=.1
N=500
Fc=.1
W=.075
T=1/W
tau=input('Enter tau: ')
noise_var=input('Enter noise variance: ')
A0 = 2/T
A1 = (2/T)*cos(pi*W*tau)
t=-50:50

for t_index=1:length(t)
t_index

f=zeros(2,N);
xterm1=zeros(1,N);
xterm2=zeros(1,N);
gterm1=zeros(1,N);
gterm2=zeros(1,N);


% Construct test signal and interpolation functions sampled at 1 Hz

for n=1:N

arg=(n-N/2)*T;

  f(1,n) = 2*W*sin(2*pi*W*(arg+tau/2)) + sqrt(noise_var)*randn(1,1);
  f(2,n) = 2*W*sin(2*pi*W*(arg-tau/2)) + sqrt(noise_var)*randn(1,1);

  xterm1(n)=(A0-A1*exp(j*2*pi*W*(arg+tau/2)))*f(1,n)/(A0^2-A1^2);
  xterm2(n)=(A0-A1*exp(j*2*pi*W*(arg-tau/2)))*f(2,n)/(A0^2-A1^2);
  gterm1(n)=W*sin(pi*W*(t(t_index)-arg-tau/2))*exp(j*pi*W*(t(t_index)-arg-
tau/2))/(pi*W*(t(t_index)-arg-tau/2));
  gterm2(n)=W*sin(pi*W*(t(t_index)-arg+tau/2))*exp(j*pi*W*(t(t_index)-
arg+tau/2))/(pi*W*(t(t_index)-arg+tau/2));

end

%for n=(N/2)+1:N
```

```
%  arg=(n-249)*T;

%  f(1,n) = 2*W*sin(2*pi*W*(arg+tau/2))/(2*pi*W*(arg+tau/2));
%  f(2,n) = 2*W*sin(2*pi*W*(arg-tau/2))/(2*pi*W*(arg-tau/2));

%  xterm1(n)=(A0-A1*exp(j*2*pi*W*(arg+tau/2)))*f(1,n)/(A0^2-A1^2);
%  xterm2(n)=(A0-A1*exp(j*2*pi*W*(arg-tau/2)))*f(2,n)/(A0^2-A1^2);
%  gterm1(n)=W*sin(pi*W*(-arg+tau/2))*exp(j*pi*W*(-arg+tau/2))/(pi*W*(-
arg+tau/2));
%  gterm2(n)=W*sin(pi*W*(-arg-tau/2))*exp(j*pi*W*(-arg-tau/2))/(pi*W*(-arg-tau/2));

%end


%f(N/2) = 2*W;
%xterm1(N/2)=(A0-A1)*f(N/2)/(A0^2-A1^2);
%xterm2(N/2)=(A0-A1)*f(N/2)/(A0^2-A1^2);
%gterm1(N/2)=W;
%gterm2(N/2)=W;



% Interpolate at .1 Hz sampling

f_hat_0=0;

for m=1:N

  f_hat_0 = f_hat_0 + xterm1(m)*gterm1(m) + xterm2(m)*gterm2(m);

end

f_hat_0_save(t_index)=2*real(f_hat_0);

%2*real(f_hat_0)

%f(1,N/2)
%f(2,N/2)

end

f_test=zeros(1,length(t));

for n=1:101
 f_test(n) = 2*W*sin(2*pi*W*t(n));
end
```

```
plot(t,f_test)
hold on
plot(t,f_hat_0_save,'.')
grid
xlabel('Time (Seconds)')
ylabel('f(t), fhat(t)')
title('Sinewave Eg, W=.075 Hz, Fs=.075 Hz, (Solid -- Original, Dots -- Reconstructed)')
```

```
% Reconstruction of 1/2 Nyquist Rate Sampled Signal
% Test Signal is the Sinc function -- Noise Simulations
% BW = .1 Hz, Sampled at .1 Hz


Fs=.1
N=500
Fc=.1
W=.1
T=1/W
tau=.1
%noise_var=input('Enter noise variance: ')
A0 = 2/T
A1 = (2/T)*cos(pi*W*tau)
b=input('Enter number of bits: ')
delta=2^-b;

for outer_loop=1:1000
outer_loop

f=zeros(2,N);
xterm1=zeros(1,N);
xterm2=zeros(1,N);
gterm1=zeros(1,N);
gterm2=zeros(1,N);


% Construct test signal and interpolation functions sampled at 1 Hz

for n=1:N

arg=(n-N/2)*T;

  f(1,n) = 2*W*sin(2*pi*W*(arg+tau/2))/(2*pi*W*(arg+tau/2)) + delta*(rand(1,1)-.5);
  f(2,n) = 2*W*sin(2*pi*W*(arg-tau/2))/(2*pi*W*(arg-tau/2)) + delta*(rand(1,1)-.5);

  xterm1(n)=(A0-A1*exp(j*2*pi*W*(arg+tau/2)))*f(1,n)/(A0^2-A1^2);
  xterm2(n)=(A0-A1*exp(j*2*pi*W*(arg-tau/2)))*f(2,n)/(A0^2-A1^2);
  gterm1(n)=W*sin(pi*W*(-arg-tau/2))*exp(j*pi*W*(-arg-tau/2))/(pi*W*(-arg-tau/2));
  gterm2(n)=W*sin(pi*W*(-arg+tau/2))*exp(j*pi*W*(-arg+tau/2))/(pi*W*(-arg+tau/2));

end

%for n=(N/2)+1:N

%  arg=(n-249)*T;
```

```
%  f(1,n) = 2*W*sin(2*pi*W*(arg+tau/2))/(2*pi*W*(arg+tau/2));
%  f(2,n) = 2*W*sin(2*pi*W*(arg-tau/2))/(2*pi*W*(arg-tau/2));

%  xterm1(n)=(A0-A1*exp(j*2*pi*W*(arg+tau/2)))*f(1,n)/(A0^2-A1^2);
%  xterm2(n)=(A0-A1*exp(j*2*pi*W*(arg-tau/2)))*f(2,n)/(A0^2-A1^2);
%  gterm1(n)=W*sin(pi*W*(-arg+tau/2))*exp(j*pi*W*(-arg+tau/2))/(pi*W*(-
arg+tau/2));
%  gterm2(n)=W*sin(pi*W*(-arg-tau/2))*exp(j*pi*W*(-arg-tau/2))/(pi*W*(-arg-tau/2));

%end


%f(N/2) = 2*W;
%xterm1(N/2)=(A0-A1)*f(N/2)/(A0^2-A1^2);
%xterm2(N/2)=(A0-A1)*f(N/2)/(A0^2-A1^2);
%gterm1(N/2)=W;
%gterm2(N/2)=W;



% Interpolate at .1 Hz sampling

f_hat_0=0;

for m=1:N

  f_hat_0 = f_hat_0 + xterm1(m)*gterm1(m) + xterm2(m)*gterm2(m);

end

f_hat_0_save(outer_loop)=2*real(f_hat_0);

2*real(f_hat_0);

%f(1,N/2)
%f(2,N/2)

end

mean(f_hat_0_save)
var(f_hat_0_save)
```

```
% Reconstruction of 1/2 Nyquist Rate Sampled Signal
% Test Signal is the Sinc function -- Quantization Noise Sims
% BW = .1 Hz, Sampled at .1 Hz


Fs=.1
N=500
Fc=.1
W=.1
T=1/W
tau=.1
%noise_var=input('Enter noise variance: ')
A0 = 2/T
A1 = (2/T)*cos(pi*W*tau)
b=input('Enter number of bits: ')
delta=2^-b;

for outer_loop=1:1000
outer_loop

f=zeros(2,N);
xterm1=zeros(1,N);
xterm2=zeros(1,N);
gterm1=zeros(1,N);
gterm2=zeros(1,N);


% Construct test signal and interpolation functions sampled at 1 Hz

for n=1:N

arg=(n-N/2)*T;

  f(1,n) = 2*W*sin(2*pi*W*(arg+tau/2))/(2*pi*W*(arg+tau/2)) + delta*(rand(1,1)-.5);
  f(2,n) = 2*W*sin(2*pi*W*(arg-tau/2))/(2*pi*W*(arg-tau/2)) + delta*(rand(1,1)-.5);

  xterm1(n)=(A0-A1*exp(j*2*pi*W*(arg+tau/2)))*f(1,n)/(A0^2-A1^2);
  xterm2(n)=(A0-A1*exp(j*2*pi*W*(arg-tau/2)))*f(2,n)/(A0^2-A1^2);
  gterm1(n)=W*sin(pi*W*(-arg-tau/2))*exp(j*pi*W*(-arg-tau/2))/(pi*W*(-arg-tau/2));
  gterm2(n)=W*sin(pi*W*(-arg+tau/2))*exp(j*pi*W*(-arg+tau/2))/(pi*W*(-arg+tau/2));

end

%for n=(N/2)+1:N

%  arg=(n-249)*T;
```

```
%  f(1,n) = 2*W*sin(2*pi*W*(arg+tau/2))/(2*pi*W*(arg+tau/2));
%  f(2,n) = 2*W*sin(2*pi*W*(arg-tau/2))/(2*pi*W*(arg-tau/2));

%  xterm1(n)=(A0-A1*exp(j*2*pi*W*(arg+tau/2)))*f(1,n)/(A0^2-A1^2);
%  xterm2(n)=(A0-A1*exp(j*2*pi*W*(arg-tau/2)))*f(2,n)/(A0^2-A1^2);
%  gterm1(n)=W*sin(pi*W*(-arg+tau/2))*exp(j*pi*W*(-arg+tau/2))/(pi*W*(-
arg+tau/2));
%  gterm2(n)=W*sin(pi*W*(-arg-tau/2))*exp(j*pi*W*(-arg-tau/2))/(pi*W*(-arg-tau/2));

%end


%f(N/2) = 2*W;
%xterm1(N/2)=(A0-A1)*f(N/2)/(A0^2-A1^2);
%xterm2(N/2)=(A0-A1)*f(N/2)/(A0^2-A1^2);
%gterm1(N/2)=W;
%gterm2(N/2)=W;



% Interpolate at .1 Hz sampling

f_hat_0=0;

for m=1:N

  f_hat_0 = f_hat_0 + xterm1(m)*gterm1(m) + xterm2(m)*gterm2(m);

end

f_hat_0_save(outer_loop)=2*real(f_hat_0);

2*real(f_hat_0);

%f(1,N/2)
%f(2,N/2)

end

mean(f_hat_0_save)
var(f_hat_0_save)
```

```
% Reconstruction of 1/2 Nyquist Rate Sampled Signal
% Test Signal is the Low Pass Noise function
% BW = .1 Hz, Sampled at .1 Hz

clf
clear

Fs=1
N=4097
W=input('Enter W: ')
T=fix(1/W)
%tau=input('Enter tau: ')
tau=2
%noise_var=input('Enter noise variance: ')
noise_var=0
A0 = 2/T
A1 = (2/T)*cos(pi*W*tau)
t=-5:5;

whitenoise=randn(1,10000);
F=[0 2*.06 2*.1 1];
A=[1 1 0 0];
b=fir2(2048,F,A);
lpnoise=filter(b,1.0,whitenoise);

f=zeros(1,N);
xterm1=zeros(1,N);
xterm2=zeros(1,N);
gterm1=zeros(1,N);
gterm2=zeros(1,N);

w=window(@hamming,N)';
f=lpnoise(7000-2048:7000+2048);

% Construct test signal and interpolation functions sampled at 1 Hz

for n=1:Fs:2048

  xterm1(n)=(A0-A1*exp(j*2*pi*W*(n-2049)))*f(n)/(A0^2-A1^2);
  xterm2(n)=(A0-A1*exp(j*2*pi*W*(n-2049)))*f(n)/(A0^2-A1^2);
  gterm1(n)=W*sin(pi*W*(2049-n))*exp(j*pi*W*(2049-n))/(pi*W*(2049-n));
  gterm2(n)=W*sin(pi*W*(2049-n))*exp(j*pi*W*(2049-n))/(pi*W*(2049-n));

end

for n=2050:Fs:4097
```

```
  xterm1(n)=(A0-A1*exp(j*2*pi*W*(n-2049)))*f(n)/(A0^2-A1^2);
  xterm2(n)=(A0-A1*exp(j*2*pi*W*(n-2049)))*f(n)/(A0^2-A1^2);
  gterm1(n)=W*sin(pi*W*(2049-n))*exp(j*pi*W*(2049-n))/(pi*W*(2049-n));
  gterm2(n)=W*sin(pi*W*(2049-n))*exp(j*pi*W*(2049-n))/(pi*W*(2049-n));

end



xterm1(2049)=(A0-A1)*f(2049)/(A0^2-A1^2);
xterm2(2049)=(A0-A1)*f(2049)/(A0^2-A1^2);
gterm1(2049)=W;
gterm2(2049)=W;



%Interpolate at .1 Hz sampling

f_hat_save=zeros(1,length(t));

for t_index=1:length(t)

    f_hat=zeros(1,length(t));

%for m = T+length(t)+1:T:N-T-length(t)
count=0;
for m = 2049-2000:T:2049+2000
count=count+1;
m_save(count)=m;

  f_hat(t_index) = f_hat(t_index) + xterm1(m+tau/2)*gterm1(t(t_index)+m+tau/2) +
xterm2(m-tau/2)*gterm2(t(t_index)+m-tau/2);

end

f_hat_save(t_index)=2*real(f_hat(t_index));

end

f_test=f(2039-fix(length(t)/2):2039+fix(length(t)/2))
f_hat_save
```

```
plot(t,f_test)
hold on
plot(t,f_hat_save,'.')
grid
xlabel('Time (Seconds)')
ylabel('f(t), fhat(t)')
title('16-QAM Eg, W=.2 Hz, Fs=.2 Hz, (Solid -- Original, Dots -- Reconstructed)')
```

```
% Reconstruction of 1/2 Nyquist Rate Sampled Signal
% Test Signal is the .25 SQRTCOS filtered 16-QAM
% BW = .2 Hz, Sampled at .2 Hz

clf
clear

Fs=1
N=4097
W=input('Enter W: ')
T=fix(1/W)
%tau=input('Enter tau: ')
tau=2
noise_var=input('Enter noise variance: ')
white_noise=sqrt(noise_var)*randn(1,N);

A0 = 2/T
A1 = (2/T)*cos(pi*W*tau)
t=-50:50;


load -MAT snr_inf.bak
qam_sig=zeros(1,N);
qam_sig(2049-1250:2049+1250)=real(MatrixData(100:2600));
w=hamming(1,2501);
%qam_sig(2049-1250:2049+1250)=w.*qam_sig(2049-1250:2049+1250);

f=zeros(1,N);
xterm1=zeros(1,N);
xterm2=zeros(1,N);
gterm1=zeros(1,N);
gterm2=zeros(1,N);

f = qam_sig + white_noise;

% Construct interpolation functions sampled at 1 Hz

for n=1:Fs:2048

  xterm1(n)=(A0-A1*exp(j*2*pi*W*(n-2049)))*f(n)/(A0^2-A1^2);
  xterm2(n)=(A0-A1*exp(j*2*pi*W*(n-2049)))*f(n)/(A0^2-A1^2);
  gterm1(n)=W*sin(pi*W*(2049-n))*exp(j*pi*W*(2049-n))/(pi*W*(2049-n));
  gterm2(n)=W*sin(pi*W*(2049-n))*exp(j*pi*W*(2049-n))/(pi*W*(2049-n));

end
```

```
for n=2050:Fs:4097

  xterm1(n)=(A0-A1*exp(j*2*pi*W*(n-2049)))*f(n)/(A0^2-A1^2);
  xterm2(n)=(A0-A1*exp(j*2*pi*W*(n-2049)))*f(n)/(A0^2-A1^2);
  gterm1(n)=W*sin(pi*W*(2049-n))*exp(j*pi*W*(2049-n))/(pi*W*(2049-n));
  gterm2(n)=W*sin(pi*W*(2049-n))*exp(j*pi*W*(2049-n))/(pi*W*(2049-n));

end



xterm1(2049)=(A0-A1)*f(2049)/(A0^2-A1^2);
xterm2(2049)=(A0-A1)*f(2049)/(A0^2-A1^2);
gterm1(2049)=W;
gterm2(2049)=W;



%Interpolate at .2 Hz sampling

f_hat_save=zeros(1,length(t));

for t_index=1:length(t)

    f_hat=zeros(1,length(t));

%for m = T+length(t)+1:T:N-T-length(t)

count=0;

for m = 2049-1250:T:2049+1250

count=count+1;

m_save(count)=m;

  f_hat(t_index) = f_hat(t_index) + xterm1(m+tau/2)*gterm1(-t(t_index)+m+tau/2) +
xterm2(m-tau/2)*gterm2(-t(t_index)+m-tau/2);

end

f_hat_save(t_index)=2*real(f_hat(t_index));

end

f_test=f(2049-fix(length(t)/2):2049+fix(length(t)/2))
```

```
f_hat_save

snr=10*log10(sum(qam_sig.^2)/noise_var)
mse=sum((f_test-f_hat_save).^2)

y=2*W*real(conv(xterm1,gterm1) + conv(xterm2,gterm2));
y(4097-fix(length(t)/2):4097+fix(length(t)/2))

plot(t,f_test)
hold on
plot(t,f_hat_save,'.')
grid
xlabel('Time (Seconds)')
ylabel('f(t), fhat(t)')
title('16-QAM Eg, W=.2 Hz, Fs=.2 Hz, (Solid -- Original, Dots -- Reconstructed)')
```

Appendix D: Random Process Reconstruction Convergence Proof in a Mean Squared Error Sense

Let $f(t)$ be a zero mean stationary random process, and $\hat{f}(t)$ be the reconstructed random process using the algorithms derived in the technical report found in Appendix A.

Although numerous simulations indicate that the reconstruction equations are valid for a random process we also desire to show the reconstruction error is zero in a mean square sense. That is we desire

$$E\left\{\left[f(t)-\hat{f}(t)\right]^2\right\}=0$$

or

$$E\left\{f^2(t)\right\}-2E\left\{f(t)\hat{f}(t)\right\}+E\left\{\hat{f}^2(t)\right\}=0.$$

Indeed we shall find that

$$E\left\{f^2(t)\right\}=E\left\{f(t)\hat{f}(t)\right\}=E\left\{\hat{f}^2(t)\right\}=R_f(0)$$

so that the reconstruction mean square error is equal to zero. We consider the three expected value functions in order.

1.) First we consider $E\left\{f^2(t)\right\}$.

By definition

$$R_f(\tau)=E\left\{f(t)f(t+\tau)\right\}$$

and with $\tau=0$ we find trivially that

$$R_f(0)=E\left\{f^2(t)\right\}.$$

2.) Secondly we consider $E\left\{f(t)\hat{f}(t)\right\}$.

It is useful to recall that an autocorrelation function can be represented as a sampling expansion since we assume the autocorrelation function is bandlimited and the random process is stationary.

Thus we may express the autocorrelation in sampled form as

$$R_f(\tau) = \sum_{n=-\infty}^{n=+\infty} R_f(nT) \frac{\sin[2\pi W(\tau - nT)]}{2\pi W(\tau - nT)}$$

or setting $\tau = 0$ we have

$$R_f(0) = \sum_{n=-\infty}^{n=+\infty} R_f(nT) \frac{\sin[2\pi W(-nT)]}{2\pi W(-nT)}.$$

We may write the reconstruction equation for $\hat{f}(t)$ as

$$\hat{f}(t) = 2\,\mathrm{Re} \sum_{n=-\infty}^{n=+\infty} \frac{A_0 - A_1 e^{j2\pi W(nT+\tau/2)}}{A_0^2 - A_1^2} f(nT + \tau/2) \frac{W \sin[\pi W(t - nT + \tau/2)]}{\pi W(t - nT + \tau/2)} e^{j\pi W(t-nT+\tau/2)}$$

$$+$$

$$\frac{A_0 - A_1 e^{j2\pi W(nT-\tau/2)}}{A_0^2 - A_1^2} f(nT - \tau/2) \frac{W \sin[\pi W(t - nT - \tau/2)]}{\pi W(t - nT - \tau/2)} e^{j\pi W(t-nT-\tau/2)}.$$

Note that

$$E\{f(t) f(nT + /- \tau/2)\} = R_f(t - nT - /+ \tau/2) = R_f(-nT - /+ \tau/2)$$

since, assuming stationarity, we may set t = 0 for convenience.

Since $f(t)$ is not a function of summation index n we may move the term inside the summation when, using the preceding equation and after moving the expectation operator inside the summation as well (expectation is a linear operation), we form

$$E\{f(t)\hat{f}(t)\} = 2\,\mathrm{Re} \sum_{n=-\infty}^{n=+\infty} R_f(-nT - \tau/2) \frac{A_0 - A_1 e^{j2\pi W(nT+\tau/2)}}{A_0^2 - A_1^2} \frac{W \sin[\pi W(-nT + \tau/2)]}{\pi W(-nT + \tau/2)} e^{j\pi W(-nT+\tau/2)}$$

$$+$$

$$R_f(-nT+\tau/2)\frac{A_0 - A_1 e^{j2\pi W(nT-\tau/2)}}{A_0^2 - A_1^2}\frac{W\sin[\pi W(-nT-\tau/2)]}{\pi W(-nT-\tau/2)}e^{j\pi W(-nT-\tau/2)}.$$

Note that this expression reconstructs $R_f(0)$ from a ½ rate sampled version of the autocorrelation function, thus we have

$$E\{f(t)\hat{f}(t)\} = R_f(0).$$

3.) We abbreviate the final exercise showing $E\{\hat{f}^2(t)\} = R_f(0)$ since the development parallels the preceding derivation which found that $E\{f(t)\hat{f}(t)\} = R_f(0)$. Additionally, the manipulations are very tedious due to the product of the two reconstruction summations. The key steps are to: (i) Replace the product of sums by a double summation of products using two summation indices such as n and k to keep the terms separate, (ii) expand the four terms created, (iii) move the expectation operator inside the double summation to form the autocorrelation functions of the form $R_f(n-k)$, (iv) then finally observe that the sinusoid products are orthogonal and sum to zero over infinity except for n=k leading to $R_f(0)$.

Then we find

$$E\{\hat{f}^2(t)\} = R_f(0).$$